The interplay between the LHC and DIS experiments in probing SMEFT

Radja Boughezal

Argonne National Laboratory

8th General Meeting of the LHC EFT Working Group

CERN, December 3, 2024

Looking for new physics @ LHC

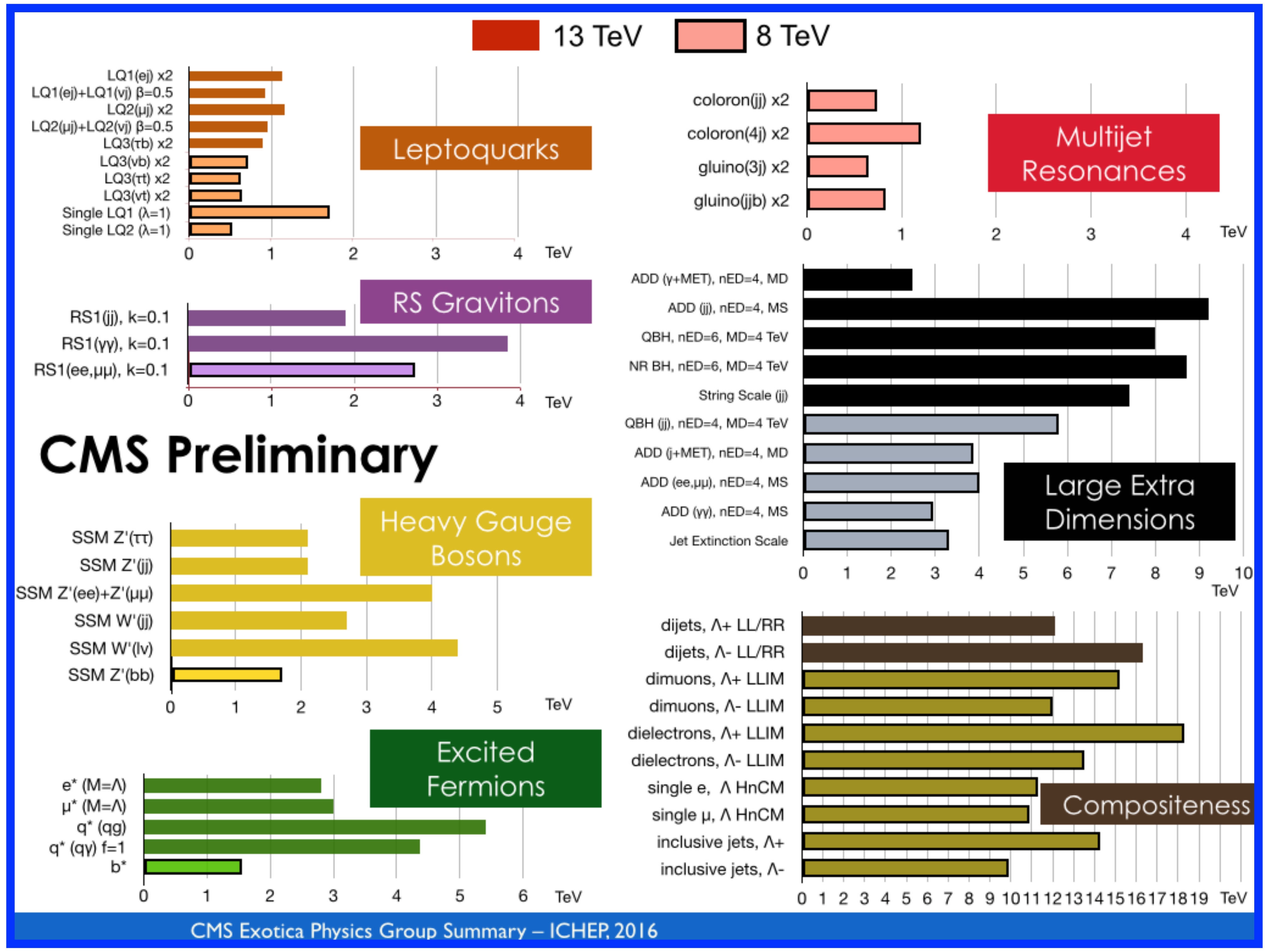

Broad model dependent searches haven't revealed new resonances so far

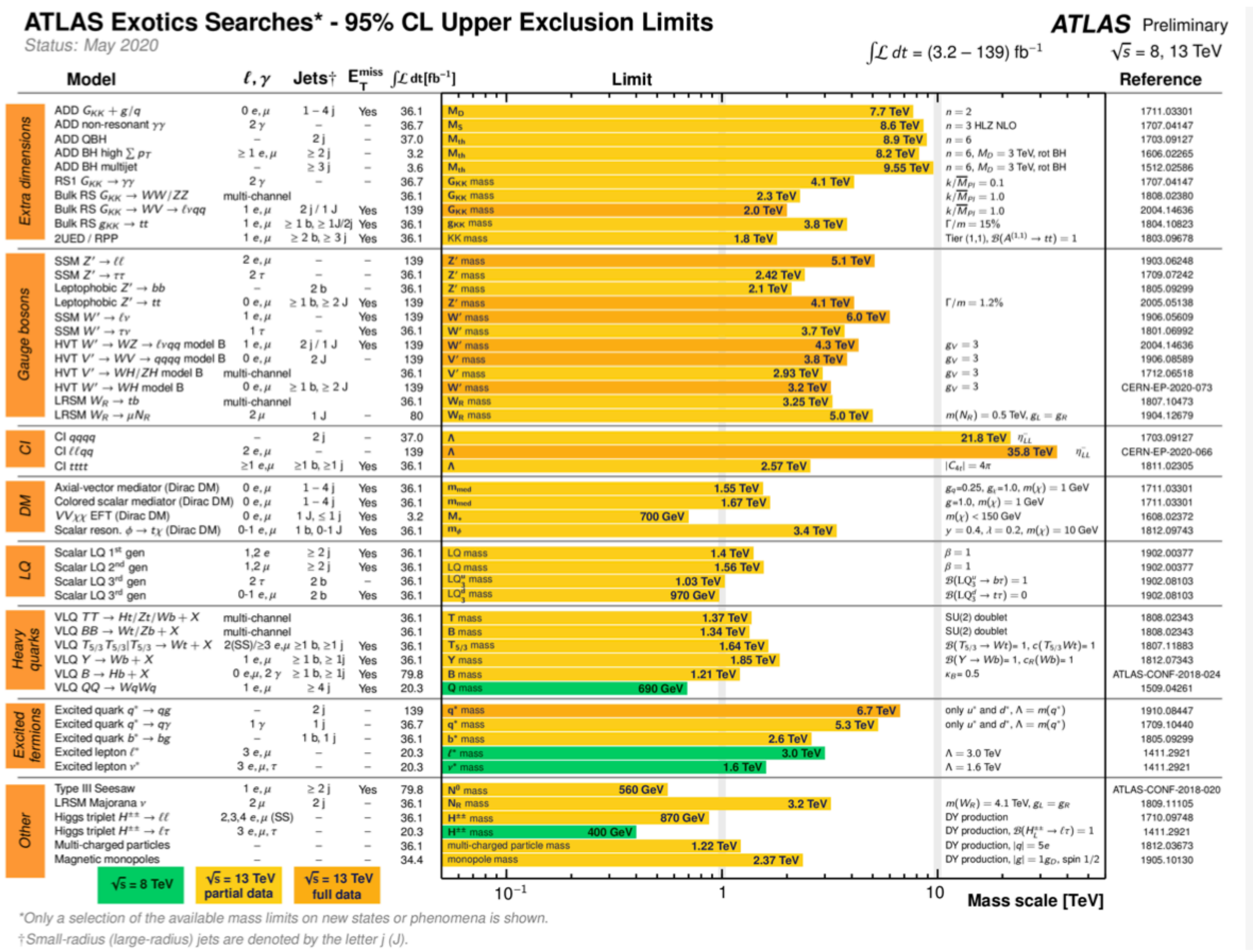

Bounds on new physics mass scale exceed several TeV in many cases

New physics might live at a scale beyond our direct colliders energy reach

Introduction to the SMEFT

- An EFT framework that incorporates this scale separation between the SM and new states is the Standard Model Effective Field Theory (SMEFT): assume the SM field content and gauge symmetry, and include all possible higher-dimensional operators suppressed by a scale Λ

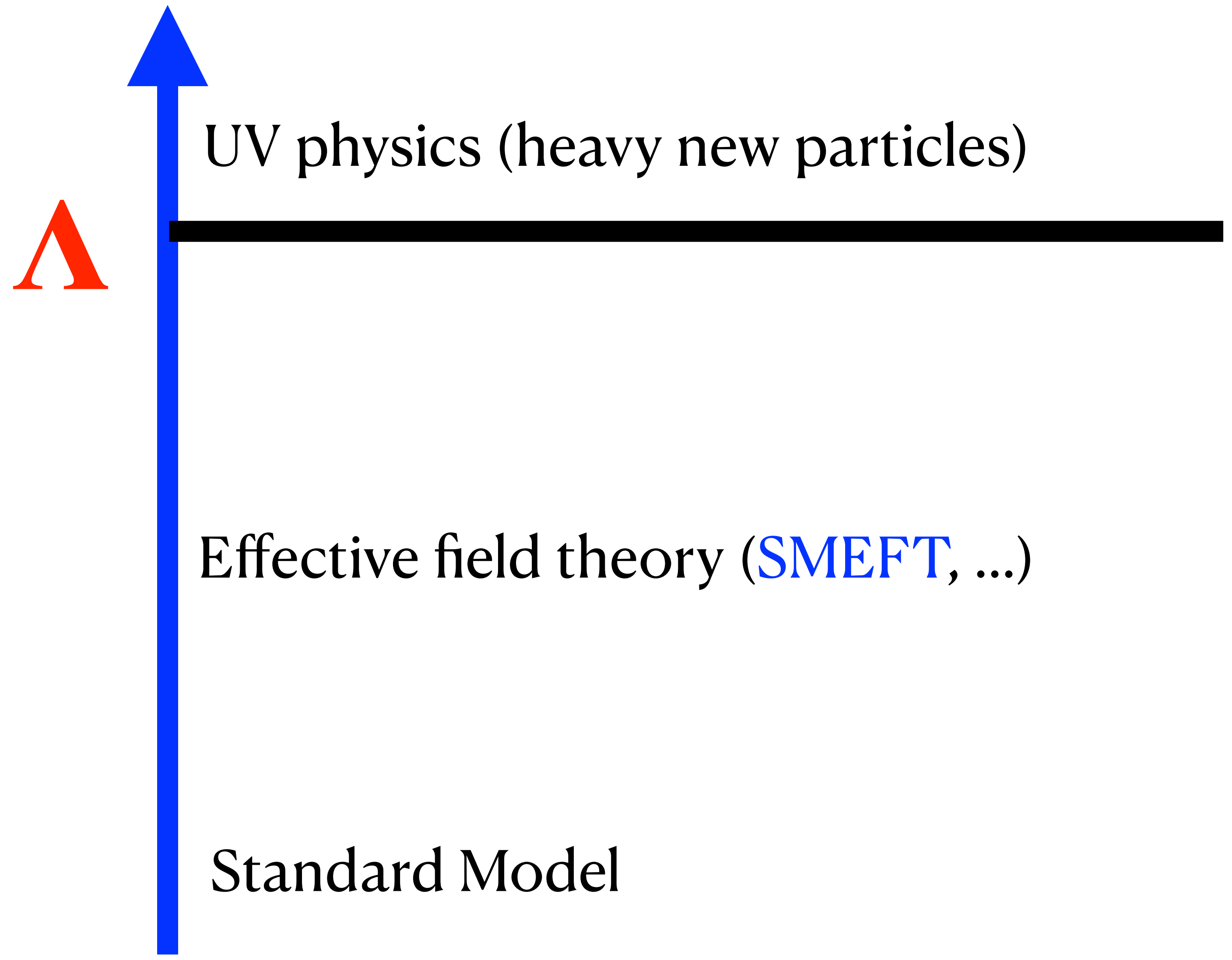

$$\mathcal{L} = \mathcal{L}_{SM} + \frac{1}{\Lambda^2}\sum_i C_6^i(\mu)\mathcal{O}_6^i(\mu) + \frac{1}{\Lambda^4}\sum_i C_8^i(\mu)\mathcal{O}_8^i(\mu) + \ldots$$

Dimension-6 Dimension-8

- $\Lambda \gg E, v$ (Higgs vev) must both be satisfied
- Odd dimensions violate lepton or baryon number; neglected here
- RG running important when comparing experiments at disparate energies

Constructing the SMEFT

- First step is to construct a complete and non-redundant basis of operators at each dimension. One commonly-used possibility at dimension-6 is the Warsaw basis.

Buchmuller, Wyler (1986); Grzadkowski et al (2010); Brivio, Jiang, Trott (2017)

Pure Gauge interactions

Accommodates a rich phenomenology in all sectors

X^3		φ^6 and $\varphi^4 D^2$		$\psi^2\varphi^3$	
Q_G	$f^{ABC} G_\mu^{A\nu} G_\nu^{B\rho} G_\rho^{C\mu}$	Q_φ	$(\varphi^\dagger\varphi)^3$	$Q_{e\varphi}$	$(\varphi^\dagger\varphi)(\bar l_p e_r \varphi)$
$Q_{\widetilde G}$	$f^{ABC} \widetilde G_\mu^{A\nu} G_\nu^{B\rho} G_\rho^{C\mu}$	$Q_{\varphi\Box}$	$(\varphi^\dagger\varphi)\Box(\varphi^\dagger\varphi)$	$Q_{u\varphi}$	$(\varphi^\dagger\varphi)(\bar q_p u_r \widetilde\varphi)$
Q_W	$\varepsilon^{IJK} W_\mu^{I\nu} W_\nu^{J\rho} W_\rho^{K\mu}$	$Q_{\varphi D}$	$\left(\varphi^\dagger D^\mu\varphi\right)^\star \left(\varphi^\dagger D_\mu\varphi\right)$	$Q_{d\varphi}$	$(\varphi^\dagger\varphi)(\bar q_p d_r \varphi)$
$Q_{\widetilde W}$	$\varepsilon^{IJK} \widetilde W_\mu^{I\nu} W_\nu^{J\rho} W_\rho^{K\mu}$				
$X^2\varphi^2$		$\psi^2 X\varphi$		$\psi^2\varphi^2 D$	
$Q_{\varphi G}$	$\varphi^\dagger \varphi\, G^A_{\mu\nu} G^{A\mu\nu}$	Q_{eW}	$(\bar l_p \sigma^{\mu\nu} e_r) \tau^I \varphi W_{\mu\nu}^I$	$Q_{\varphi l}^{(1)}$	$(\varphi^\dagger i\overleftrightarrow{D}_\mu \varphi)(\bar l_p \gamma^\mu l_r)$
$Q_{\varphi\widetilde G}$	$\varphi^\dagger \varphi\, \widetilde G^A_{\mu\nu} G^{A\mu\nu}$	Q_{eB}	$(\bar l_p \sigma^{\mu\nu} e_r) \varphi B_{\mu\nu}$	$Q_{\varphi l}^{(3)}$	$(\varphi^\dagger i\overleftrightarrow{D}^I_\mu \varphi)(\bar l_p \tau^I \gamma^\mu l_r)$
$Q_{\varphi W}$	$\varphi^\dagger \varphi\, W^I_{\mu\nu} W^{I\mu\nu}$	Q_{uG}	$(\bar q_p \sigma^{\mu\nu} T^A u_r) \widetilde\varphi\, G_{\mu\nu}^A$	$Q_{\varphi e}$	$(\varphi^\dagger i\overleftrightarrow{D}_\mu \varphi)(\bar e_p \gamma^\mu e_r)$
$Q_{\varphi\widetilde W}$	$\varphi^\dagger \varphi\, \widetilde W^I_{\mu\nu} W^{I\mu\nu}$	Q_{uW}	$(\bar q_p \sigma^{\mu\nu} u_r) \tau^I \widetilde\varphi\, W_{\mu\nu}^I$	$Q_{\varphi q}^{(1)}$	$(\varphi^\dagger i\overleftrightarrow{D}_\mu \varphi)(\bar q_p \gamma^\mu q_r)$
$Q_{\varphi B}$	$\varphi^\dagger \varphi\, B_{\mu\nu} B^{\mu\nu}$	Q_{uB}	$(\bar q_p \sigma^{\mu\nu} u_r) \widetilde\varphi\, B_{\mu\nu}$	$Q_{\varphi q}^{(3)}$	$(\varphi^\dagger i\overleftrightarrow{D}^I_\mu \varphi)(\bar q_p \tau^I \gamma^\mu q_r)$
$Q_{\varphi\widetilde B}$	$\varphi^\dagger \varphi\, \widetilde B_{\mu\nu} B^{\mu\nu}$	Q_{dG}	$(\bar q_p \sigma^{\mu\nu} T^A d_r) \varphi\, G_{\mu\nu}^A$	$Q_{\varphi u}$	$(\varphi^\dagger i\overleftrightarrow{D}_\mu \varphi)(\bar u_p \gamma^\mu u_r)$
$Q_{\varphi WB}$	$\varphi^\dagger \tau^I \varphi\, W^I_{\mu\nu} B^{\mu\nu}$	Q_{dW}	$(\bar q_p \sigma^{\mu\nu} d_r) \tau^I \varphi\, W_{\mu\nu}^I$	$Q_{\varphi d}$	$(\varphi^\dagger i\overleftrightarrow{D}_\mu \varphi)(\bar d_p \gamma^\mu d_r)$
$Q_{\varphi\widetilde WB}$	$\varphi^\dagger \tau^I \varphi\, \widetilde W^I_{\mu\nu} B^{\mu\nu}$	Q_{dB}	$(\bar q_p \sigma^{\mu\nu} d_r) \varphi\, B_{\mu\nu}$	$Q_{\varphi ud}$	$i(\widetilde\varphi^\dagger D_\mu \varphi)(\bar u_p \gamma^\mu d_r)$

$(\bar LL)(\bar LL)$		$(\bar RR)(\bar RR)$		$(\bar LL)(\bar RR)$	
Q_{ll}	$(\bar l_p \gamma_\mu l_r)(\bar l_s \gamma^\mu l_t)$	Q_{ee}	$(\bar e_p \gamma_\mu e_r)(\bar e_s \gamma^\mu e_t)$	Q_{le}	$(\bar l_p \gamma_\mu l_r)(\bar e_s \gamma^\mu e_t)$
$Q_{qq}^{(1)}$	$(\bar q_p \gamma_\mu q_r)(\bar q_s \gamma^\mu q_t)$	Q_{uu}	$(\bar u_p \gamma_\mu u_r)(\bar u_s \gamma^\mu u_t)$	Q_{lu}	$(\bar l_p \gamma_\mu l_r)(\bar u_s \gamma^\mu u_t)$
$Q_{qq}^{(3)}$	$(\bar q_p \gamma_\mu \tau^I q_r)(\bar q_s \gamma^\mu \tau^I q_t)$	Q_{dd}	$(\bar d_p \gamma_\mu d_r)(\bar d_s \gamma^\mu d_t)$	Q_{ld}	$(\bar l_p \gamma_\mu l_r)(\bar d_s \gamma^\mu d_t)$
$Q_{lq}^{(1)}$	$(\bar l_p \gamma_\mu l_r)(\bar q_s \gamma^\mu q_t)$	Q_{eu}	$(\bar e_p \gamma_\mu e_r)(\bar u_s \gamma^\mu u_t)$	Q_{qe}	$(\bar q_p \gamma_\mu q_r)(\bar e_s \gamma^\mu e_t)$
$Q_{lq}^{(3)}$	$(\bar l_p \gamma_\mu \tau^I l_r)(\bar q_s \gamma^\mu \tau^I q_t)$	Q_{ed}	$(\bar e_p \gamma_\mu e_r)(\bar d_s \gamma^\mu d_t)$	$Q_{qu}^{(1)}$	$(\bar q_p \gamma_\mu q_r)(\bar u_s \gamma^\mu u_t)$
		$Q_{ud}^{(1)}$	$(\bar u_p \gamma_\mu u_r)(\bar d_s \gamma^\mu d_t)$	$Q_{qu}^{(8)}$	$(\bar q_p \gamma_\mu T^A q_r)(\bar u_s \gamma^\mu T^A u_t)$
		$Q_{ud}^{(8)}$	$(\bar u_p \gamma_\mu T^A u_r)(\bar d_s \gamma^\mu T^A d_t)$	$Q_{qd}^{(1)}$	$(\bar q_p \gamma_\mu q_r)(\bar d_s \gamma^\mu d_t)$
				$Q_{qd}^{(8)}$	$(\bar q_p \gamma_\mu T^A q_r)(\bar d_s \gamma^\mu T^A d_t)$
$(\bar LR)(\bar RL)$ and $(\bar LR)(\bar LR)$		B-violating			
Q_{ledq}	$(\bar l_p^j e_r)(\bar d_s q_t^j)$	Q_{duq}	$\varepsilon^{\alpha\beta\gamma}\varepsilon_{jk}\left[(d_p^\alpha)^T C u_r^\beta\right]\left[(q_s^{\gamma j})^T C l_t^k\right]$		
$Q_{quqd}^{(1)}$	$(\bar q_p^j u_r)\varepsilon_{jk}(\bar q_s^k d_t)$	Q_{qqu}	$\varepsilon^{\alpha\beta\gamma}\varepsilon_{jk}\left[(q_p^{\alpha j})^T C q_r^{\beta k}\right]\left[(u_s^\gamma)^T C e_t\right]$		
$Q_{quqd}^{(8)}$	$(\bar q_p^j T^A u_r)\varepsilon_{jk}(\bar q_s^k T^A d_t)$	Q_{qqq}	$\varepsilon^{\alpha\beta\gamma}\varepsilon_{jn}\varepsilon_{km}\left[(q_p^{\alpha j})^T C q_r^{\beta k}\right]\left[(q_s^{\gamma m})^T C l_t^n\right]$		
$Q_{lequ}^{(1)}$	$(\bar l_p^j e_r)\varepsilon_{jk}(\bar q_s^k u_t)$	Q_{duu}	$\varepsilon^{\alpha\beta\gamma}\left[(d_p^\alpha)^T C u_r^\beta\right]\left[(u_s^\gamma)^T C e_t\right]$		
$Q_{lequ}^{(3)}$	$(\bar l_p^j \sigma_{\mu\nu} e_r)\varepsilon_{jk}(\bar q_s^k \sigma^{\mu\nu} u_t)$				

Gauge-Higgs interactions

Fermion-Higgs-gauge interactions

Four-fermion interactions

Baryon-number violating interactions

Constructing the SMEFT

- First step is to construct a complete and non-redundant basis of operators at each dimension. One commonly-used possibility at dimension-6 is the Warsaw basis.

Buchmuller, Wyler (1986); Grzadkowski et al (2010); Brivio, Jiang, Trott (2017)

Pure Gauge interactions

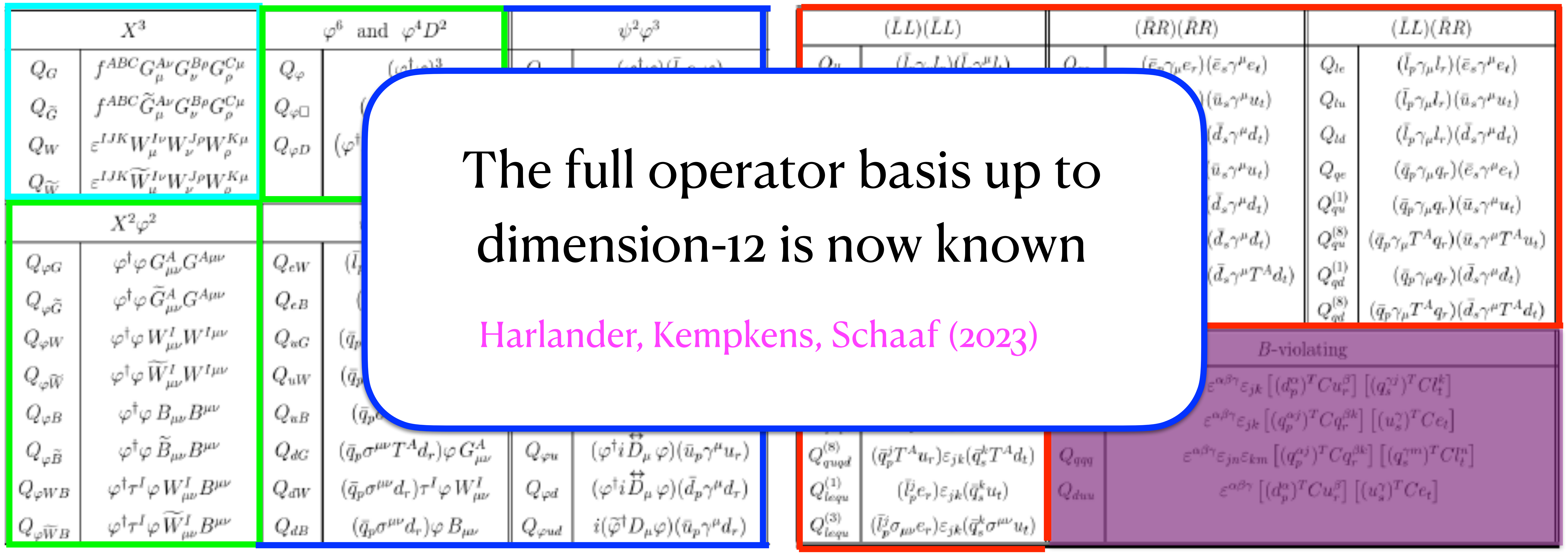

The full operator basis up to dimension-12 is now known

Harlander, Kempkens, Schaaf (2023)

Gauge-Higgs interactions

Fermion-Higgs-gauge interactions

Four-fermion interactions

Baryon-number violating interactions

Searching for the SMEFT

- The most natural experiments to look for SMEFT-induced deviations are high-energy ones such as the LHC, since the expansion parameter C^*E^2/Λ^2 is maximized there. Global fits to the available data are pursued by both the experimental and theoretical collaborations.

One example: Ellis et al (2020)

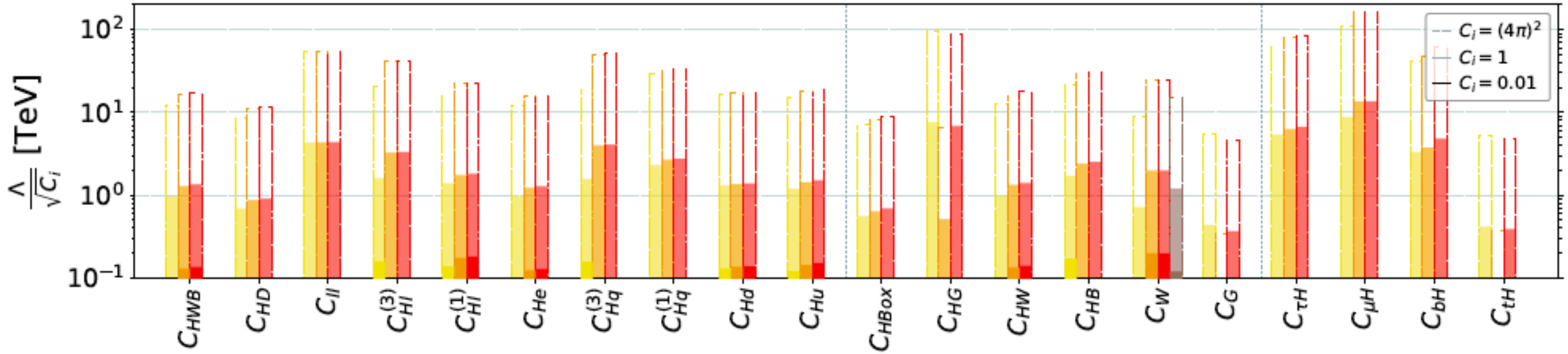

The LHC provides a rich program to search for a broad spectrum of coefficients to the TeV scale; we'll focus first on an example sector of SMEFT here

SMEFT probes at the LHC

Example: semi-leptonic four-fermion operators

- We will study in detail the LHC example of semi-leptonic four-fermion operators in the SMEFT. These are the relevant operators for models containing states such as Z' bosons and gravitons. The natural place to search for them at the LHC is through the Drell-Yan process at high energies.

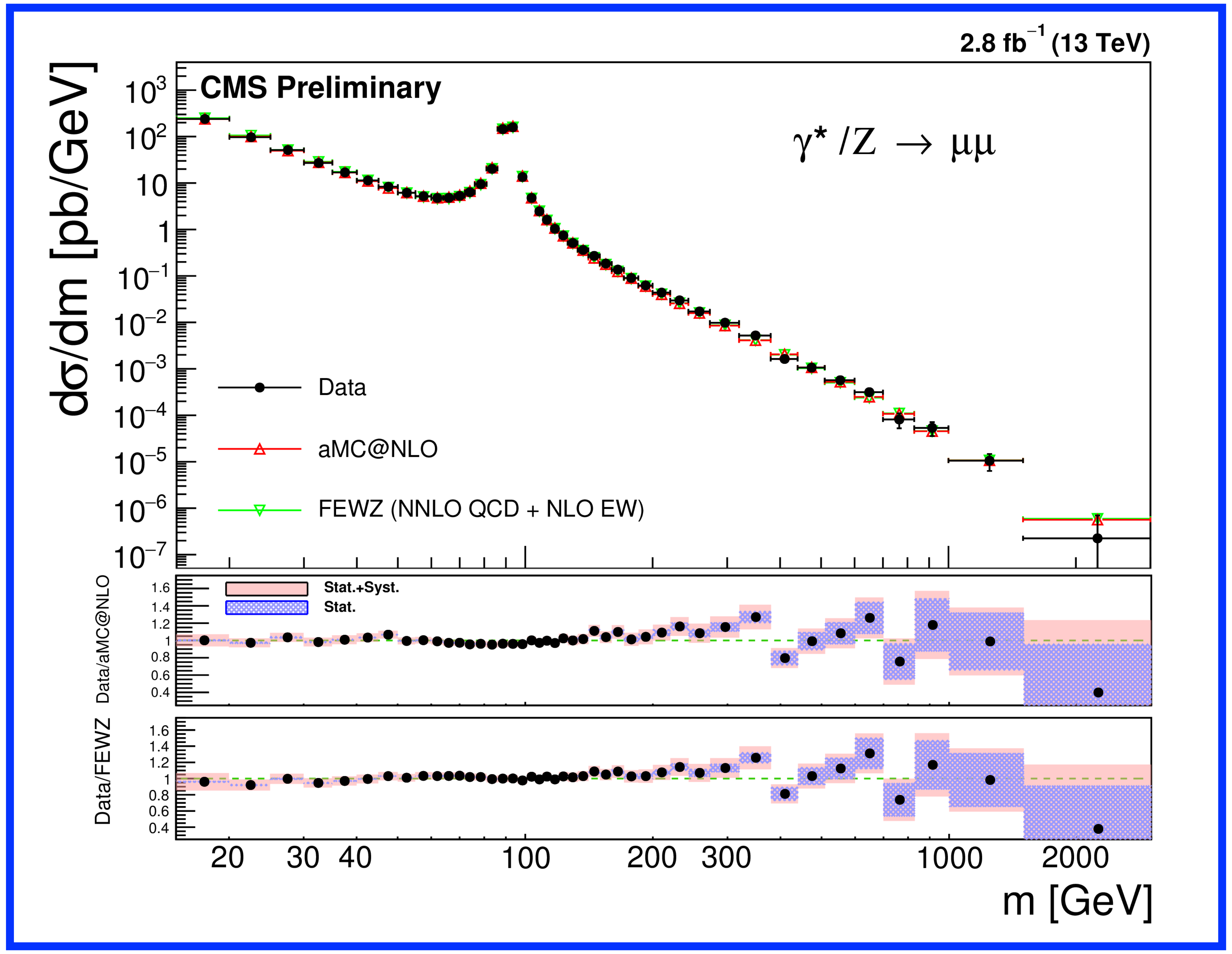

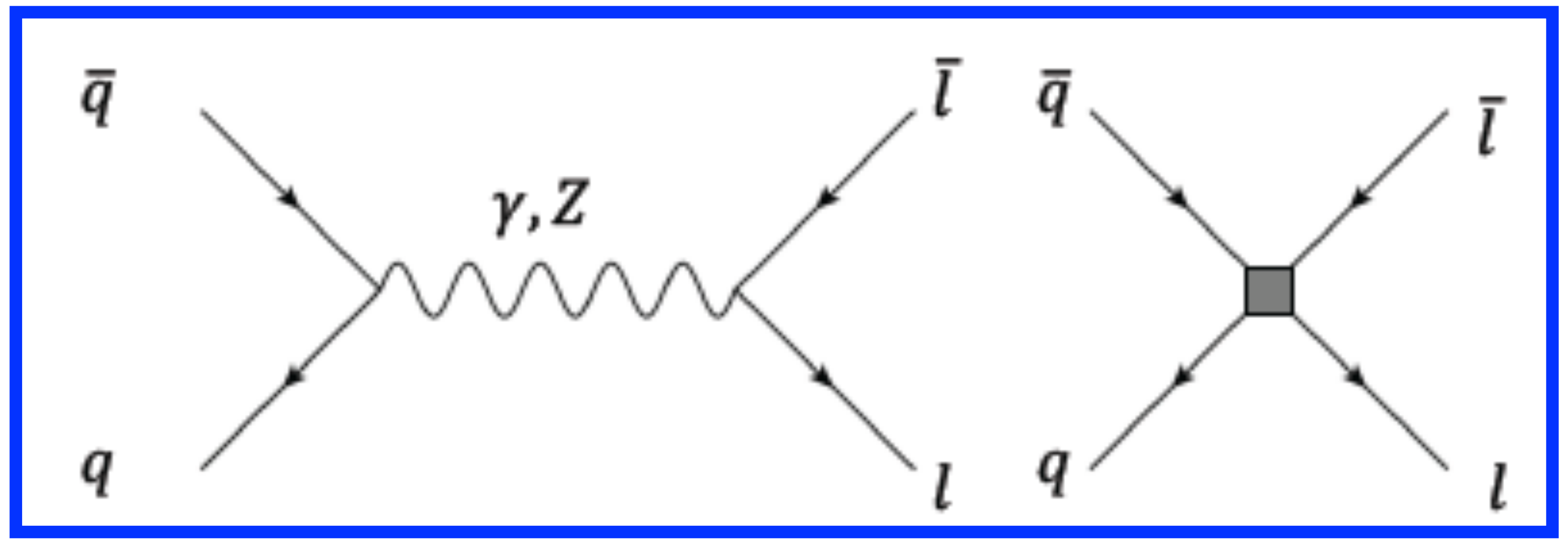

Both data and theory are precise up to high invariant masses

For additional SMEFT DY studies see also: Panico, Ricci, Wulzer (2021); Allwicher et al (2022)

Operator basis

- The relevant four-fermion operators consist of 7 dim-6 and 14 dim-8 operators.

Dimension 6		Dimension 8	
$\mathcal{O}_{lq}^{(1)}$	$(\bar{l}\gamma^\mu l)(\bar{q}\gamma_\mu q)$	$\mathcal{O}_{l^2q^2D^2}^{(1)}$	$D^\nu(\bar{l}\gamma^\mu l)D_\nu(\bar{q}\gamma_\mu q)$
$\mathcal{O}_{lq}^{(3)}$	$(\bar{l}\gamma^\mu\tau^i l)(\bar{q}\gamma_\mu\tau^i q)$	$\mathcal{O}_{l^2q^2D^2}^{(3)}$	$D^\nu(\bar{l}\gamma^\mu\tau^i l)D_\nu(\bar{q}\gamma_\mu\tau^i q)$
$\mathcal{O}_{eu}$	$(\bar{e}\gamma^\mu e)(\bar{u}\gamma_\mu u)$	$\mathcal{O}_{e^2u^2D^2}^{(1)}$	$D^\nu(\bar{e}\gamma^\mu e)D_\nu(\bar{u}\gamma_\mu u)$
$\mathcal{O}_{ed}$	$(\bar{e}\gamma^\mu e)(\bar{d}\gamma_\mu d)$	$\mathcal{O}_{e^2d^2D^2}^{(1)}$	$D^\nu(\bar{e}\gamma^\mu e)D_\nu(\bar{d}\gamma_\mu d)$
$\mathcal{O}_{lu}$	$(\bar{l}\gamma^\mu l)(\bar{u}\gamma_\mu u)$	$\mathcal{O}_{l^2u^2D^2}^{(1)}$	$D^\nu(\bar{l}\gamma^\mu l)D_\nu(\bar{u}\gamma_\mu u)$
$\mathcal{O}_{ld}$	$(\bar{l}\gamma^\mu l)(\bar{d}\gamma_\mu d)$	$\mathcal{O}_{l^2d^2D^2}^{(1)}$	$D^\nu(\bar{l}\gamma^\mu l)D_\nu(\bar{d}\gamma_\mu d)$
$\mathcal{O}_{qe}$	$(\bar{q}\gamma^\mu q)(\bar{e}\gamma_\mu e)$	$\mathcal{O}_{q^2e^2D^2}^{(1)}$	$D^\nu(\bar{q}\gamma^\mu q)D_\nu(\bar{e}\gamma_\mu e)$

Dimension 8

$$\mathcal{O}_{8,ed\partial 2} = (\bar{e}\gamma_\mu \overleftrightarrow{D}_\nu e)(\bar{d}\gamma^\mu \overleftrightarrow{D}^\nu d),$$
$$\mathcal{O}_{8,eu\partial 2} = (\bar{e}\gamma_\mu \overleftrightarrow{D}_\nu e)(\bar{u}\gamma^\mu \overleftrightarrow{D}^\nu u),$$
$$\mathcal{O}_{8,ld\partial 2} = (\bar{l}\gamma_\mu \overleftrightarrow{D}_\nu l)(\bar{d}\gamma^\mu \overleftrightarrow{D}^\nu d),$$
$$\mathcal{O}_{8,lu\partial 2} = (\bar{l}\gamma_\mu \overleftrightarrow{D}_\nu l)(\bar{u}\gamma^\mu \overleftrightarrow{D}^\nu u),$$
$$\mathcal{O}_{8,qe\partial 2} = (\bar{e}\gamma_\mu \overleftrightarrow{D}_\nu e)(\bar{q}\gamma^\mu \overleftrightarrow{D}^\nu q).$$
$$\mathcal{O}_{8,lq\partial 3} = (\bar{l}\gamma_\mu \overleftrightarrow{D}_\nu l)(\bar{q}\gamma^\mu \overleftrightarrow{D}^\nu q),$$
$$\mathcal{O}_{8,lq\partial 4} = (\bar{l}\tau^I\gamma_\mu \overleftrightarrow{D}_\nu l)(\bar{q}\tau^I\gamma^\mu \overleftrightarrow{D}^\nu q)$$

Relevant operators for our analysis; note q,l are left-handed doublets; e,u,d are right-handed singlets

Operator basis

- The relevant four-fermion operators consist of seven dim-6 and 14 dim-8 operators.

$$O_{\varphi\ell}^{(1)} = (\varphi^\dagger i \overleftrightarrow{D}_\mu \varphi)(\bar{\ell}\gamma^\mu \ell)$$
$$O_{\varphi\ell}^{(3)} = (\varphi^\dagger i \overleftrightarrow{D}_\mu \tau^I \varphi)(\bar{\ell}\gamma^\mu \tau^I \ell)$$
$$O_{\varphi e} = (\varphi^\dagger i \overleftrightarrow{D}_\mu \varphi)(\bar{e}\gamma^\mu e)$$
$$O_{\varphi q}^{(1)} = (\varphi^\dagger i \overleftrightarrow{D}_\mu \varphi)(\bar{q}\gamma^\mu q)$$
$$O_{\varphi q}^{(3)} = (\varphi^\dagger i \overleftrightarrow{D}_\mu \tau^I \varphi)(\bar{q}\gamma^\mu \tau^I q)$$
$$O_{\varphi u} = (\varphi^\dagger i \overleftrightarrow{D}_\mu \varphi)(\bar{u}\gamma^\mu u)$$
$$O_{\varphi d} = (\varphi^\dagger i \overleftrightarrow{D}_\mu \varphi)(\bar{d}\gamma^\mu d)$$

Dawson, Giardino (2019)

C_k	95% CL, $\Lambda = 1$ TeV
$C_{\varphi\ell}^{(1)}$	$[-0.043, 0.012]$
$C_{\varphi\ell}^{(3)}$	$[-0.012, 0.0029]$
$C_{\varphi e}$	$[-0.013, 0.0094]$
$C_{\varphi q}^{(1)}$	$[-0.027, 0.043]$
$C_{\varphi q}^{(3)}$	$[-0.011, 0.014]$
$C_{\varphi u}$	$[-0.072, 0.091]$
$C_{\varphi d}$	$[-0.16, 0.060]$
$C_{\varphi WB}$	$[-0.0088, 0.0013]$

Other operators contribute as well, and shift the ffV vertices

These are better constrained by the precision Z-pole data of LEP, SLC; however, these experiments only weakly constrain four-fermion operators

Invariant mass and A_{FB} constraints

- We study constraints from existing data sets: invariant mass distributions and forward-backward asymmetries. Measurements at 13 TeV correspond to high integrated luminosity. The relevant data sets from ATLAS and CMS are summarized below.

No.	Experiment	$\sqrt{s}$	Measurement	Luminosity	m_{ll}^{low}	Ref.
I	ATLAS	8 TeV	$d\sigma/dm$	20.3 fb^{-1}	116-1000 GeV	[24]
II	CMS	13 TeV	$d\sigma/dm$	137 fb^{-1} (ee) 140 fb^{-1} $(\mu\mu)$	200-2210 GeV (ee) 210-2290 GeV $(\mu\mu)$	[25]
III	CMS	8 TeV	A^*_{FB}	19.7 fb^{-1}	120-500 GeV	[26]
IV	CMS	13 TeV	A_{FB}	138 fb^{-1}	170-1000 GeV	[27]

Excellent test case for how well LHC covers the SMEFT; significant high-luminosity, high-quality data

Single parameter vs. marginalized fits

- We begin with a fit to the linear dimension-6 SMEFT basis. There are seven relevant semi-leptonic four-fermion Wilson coefficients with this assumption. We first consider single-parameter versus marginalized fits

RB, Huang, Petriello (2023)

Dimension 6	
$\mathcal{O}_{lq}^{(1)}$	$(\bar{l}\gamma^\mu l)\,(\bar{q}\gamma_\mu q)$
$\mathcal{O}_{lq}^{(3)}$	$(\bar{l}\gamma^\mu \tau^i l)\,(\bar{q}\gamma_\mu \tau^i q)$
$\mathcal{O}_{eu}$	$(\bar{e}\gamma^\mu e)\,(\bar{u}\gamma_\mu u)$
$\mathcal{O}_{ed}$	$(\bar{e}\gamma^\mu e)\,(\bar{d}\gamma_\mu d)$
$\mathcal{O}_{lu}$	$(\bar{l}\gamma^\mu l)\,(\bar{u}\gamma_\mu u)$
$\mathcal{O}_{ld}$	$(\bar{l}\gamma^\mu l)\,(\bar{d}\gamma_\mu d)$
$\mathcal{O}_{qe}$	$(\bar{q}\gamma^\mu q)\,(\bar{e}\gamma_\mu e)$

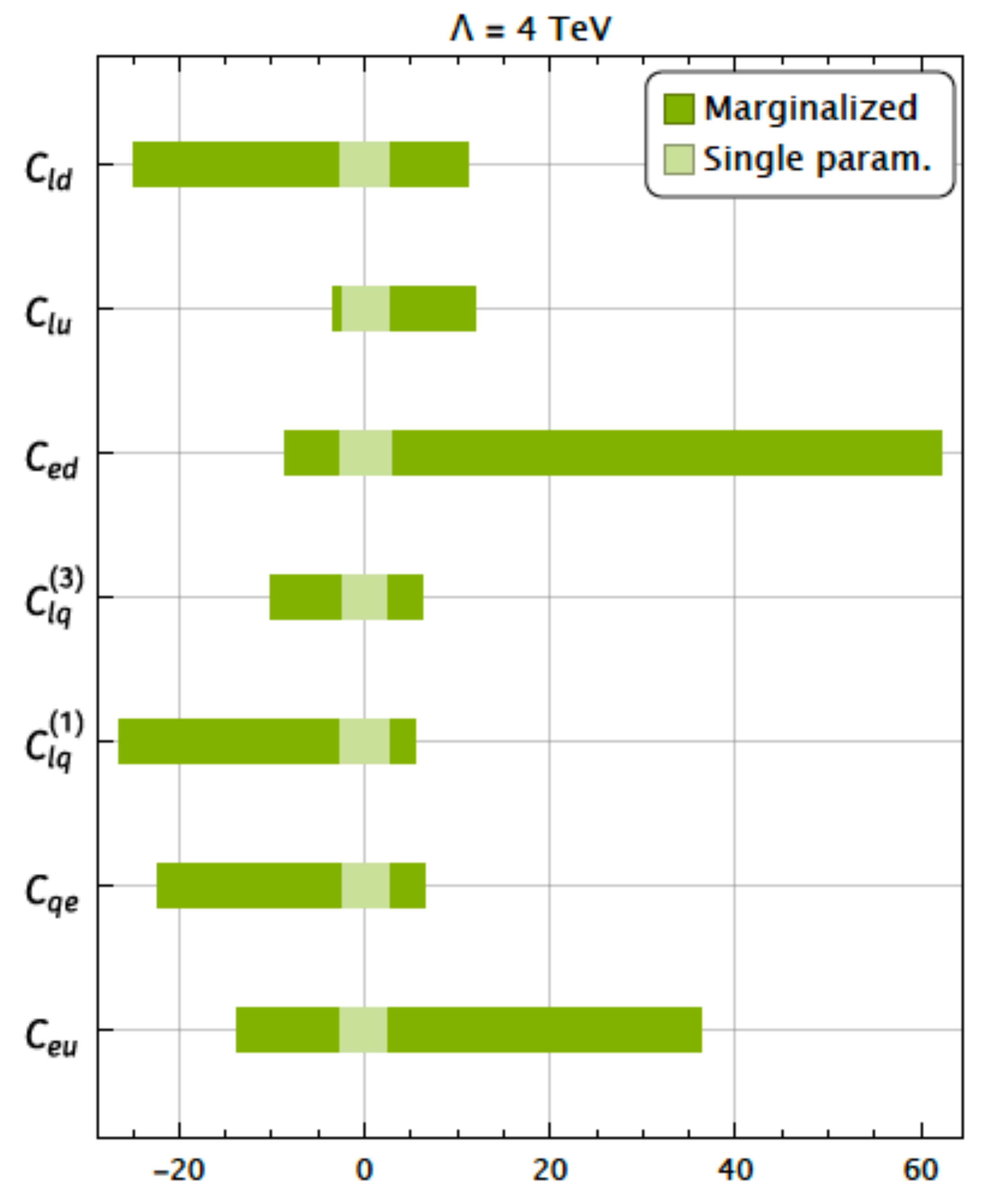

There is a significant difference between the single-parameter and marginalized fits, indicating the need to turn all Wilson coefficients on simultaneously

Linear vs. quadratic fits

- We now consider the difference between expanding the dimension-6 SMEFT corrections to both linear and quadratic orders. As an example we will turn on two coefficients only.

RB, Huang, Petriello (2023)

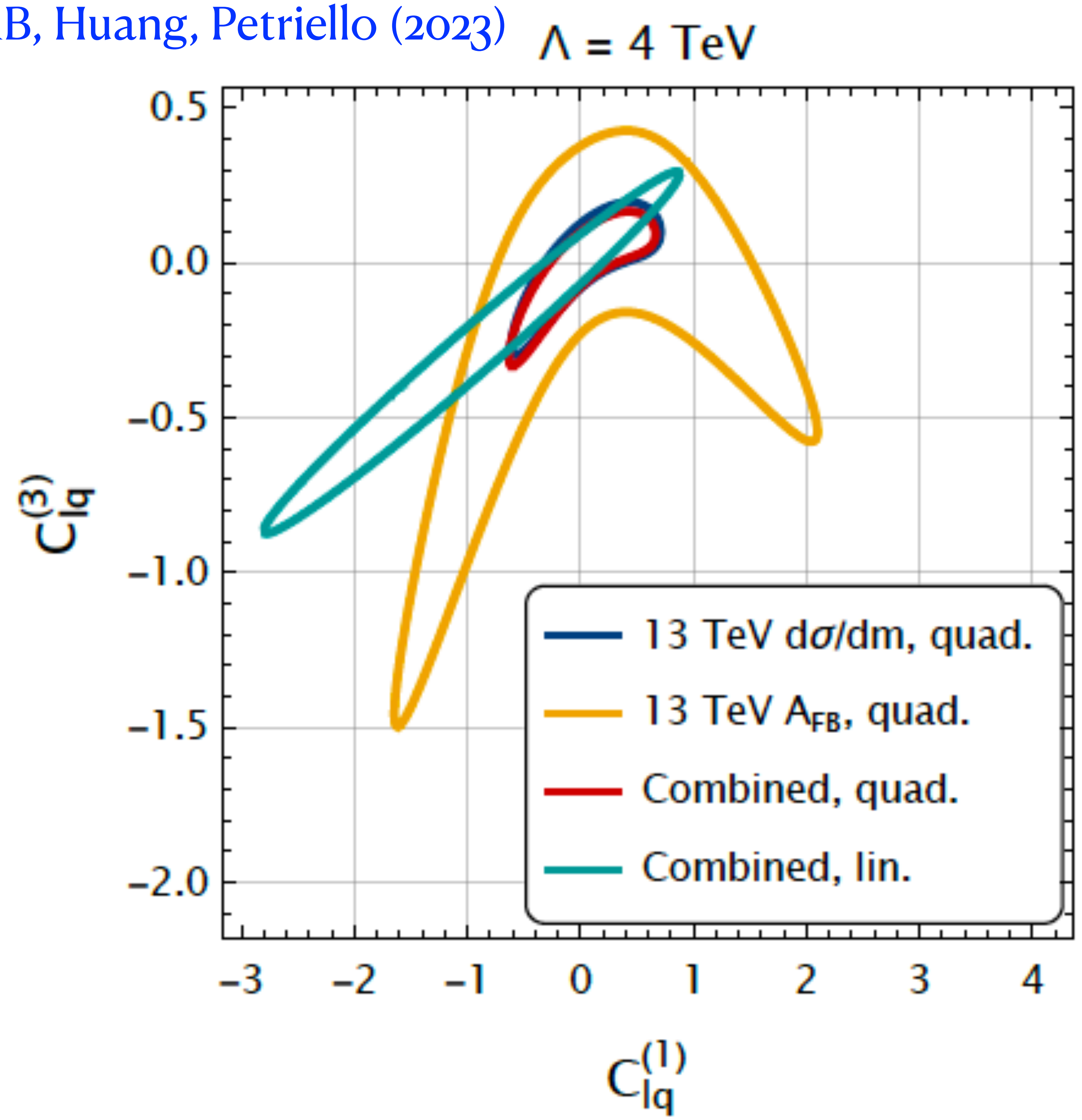

- The A_{FB} data set (boomerang shape) alone exhibits significant degeneracies; need to fit to multiple data sets!
- Linear (cyan) and quadratic (red) combined fits differ significantly; important to include higher-order terms in the SMEFT expansion!
- Note that A_{FB} data doesn't improve the combined fit; the power comes from the invariant mass data

Dimension-8 effects

- If quadratic dimension-6 terms have an effect, dimension-8 terms should as well.

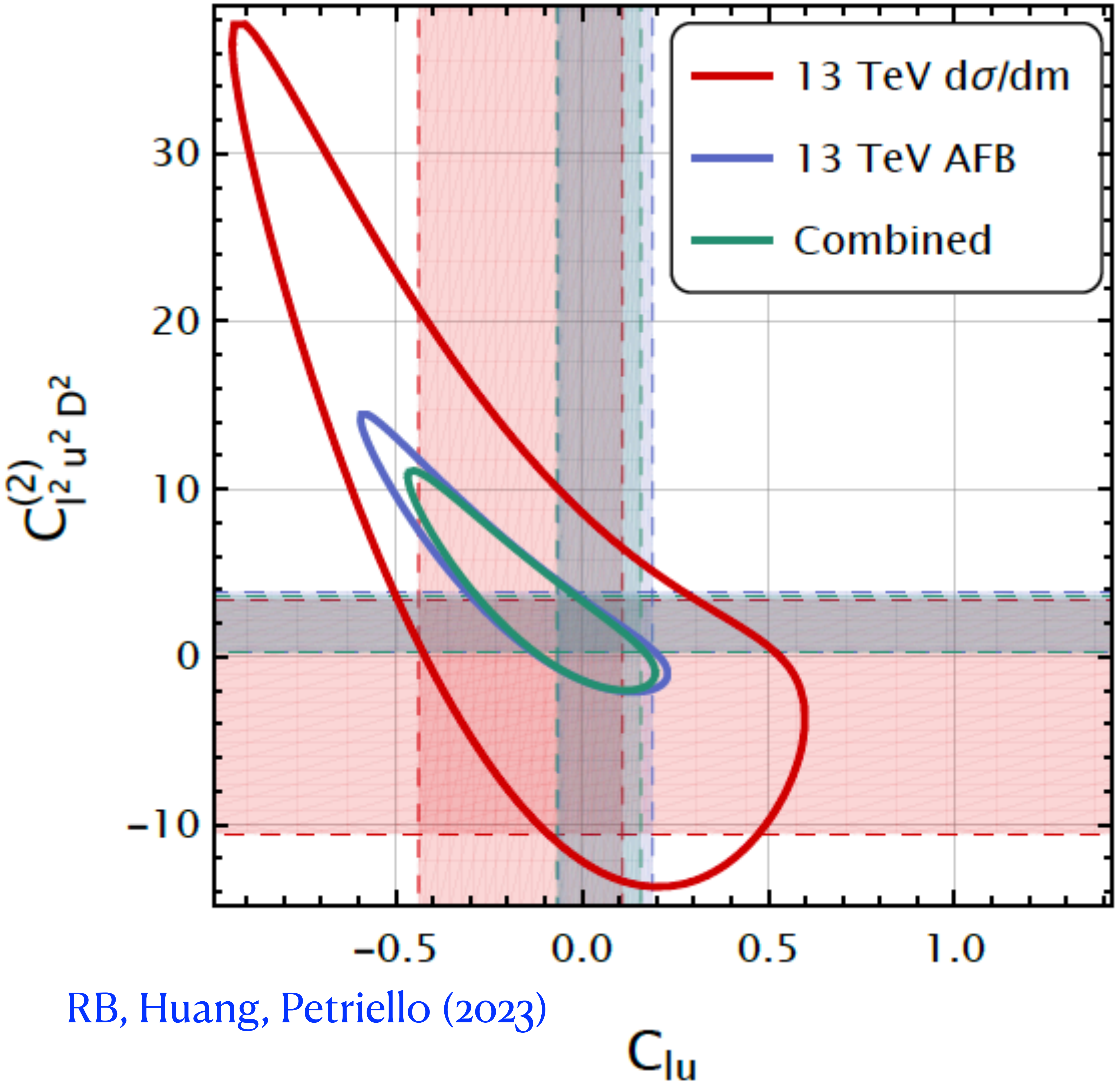

RB, Huang, Petriello (2023)

- Turn on left-handed lepton coupling to right handed up quark at dim-6 and dim-8 as an example.
- Shaded regions are the one-parameter constraints at 95% CL. Ellipses are when both parameters are turned on.
- Significant shifts! For example, the allowed region of C_{lu} extends to -0.5 with dim-8 turned on; in the single parameter fit it extends only to -0.1.
- Note this time constraints primarily from A_{FB}!
- RG running has minimal impact on these fits RB, Huang, Petriello (2024)

This is with all the relevant LHC DY data!

What have we learned so far?

- Single-parameter fits give bounds significantly different than those obtained from a full fit.
- The use of all available data is needed to help reduce degeneracies in the parameter space.
- Quadratic dimension-6 terms can have an important impact on SMEFT fits.
- Dimension-8 terms can have an important effect in fits (this is model-dependent: studies with certain *Z'* models matched to SMEFT indicate little impact from dimension-8 effects RB, Huang, Petriello (2024); Dawson, Forslund, Schnubel (2024))

The LHC alone isn't enough to fully cover the parameter space, degeneracies exist between dim6 coefficients themselves and between dim6 and dim8.

Future electron-hadron experiments

- Another possibility of probing the SMEFT parameter space is with future DIS experiments. These are sensitive to the same operators as Drell-Yan. A host of facilities spanning low and high energies are planned for both the near and far future.

High energy DIS:

- Electron-Ion Collider (EIC): $\sqrt{s}$~140 GeV
- Future Circular Collider (FCC-eh): $\sqrt{s}$~3.4 TeV
- Large Hadron Electron Collider (LHeC): $\sqrt{s}$~1.3 TeV

Low energy PVES:

- Solenoidal Large Inensity Device (SoLID) at Jlab ($2<Q^2<10\,\mathrm{GeV}^2$, electron-deuteron scattering)
- P2 at Mainz (155 MeV electrons off hydrogen/carbon targets)

A key feature shared by all of these experiments is the ability to polarize beams; a key distinction from the LHC!

$$\frac{d^2\sigma_u^{\gamma SMEFT}}{dx dQ^2} = -x\frac{Q_u Q^2}{8\pi\alpha}\Big[C_{eu}(1+\lambda_u)(1+\lambda_e) + (C_{lq}^{(1)} - C_{lq}^{(3)})(1-\lambda_u)(1-\lambda_e) +(1-y)^2 C_{lu}(1+\lambda_u)(1-\lambda_e) + (1-y)^2 C_{qe}(1-\lambda_u)(1+\lambda_e)\Big]$$

Disentangle Wilson coefficients with polarization

SMEFT probes at the EIC

Key features of the EIC

- In our analysis of SMEFT at the EIC we assume the following run parameters:

Deuteron beam: Proton beam:

D1	5 GeV $\times$ 41 GeV eD, 4.4 fb^{-1}	P1	5 GeV $\times$ 41 GeV ep, 4.4 fb^{-1}
D2	5 GeV $\times$ 100 GeV eD, 36.8 fb^{-1}	P2	5 GeV $\times$ 100 GeV ep, 36.8 fb^{-1}
D3	10 GeV $\times$ 100 GeV eD, 44.8 fb^{-1}	P3	10 GeV $\times$ 100 GeV ep, 44.8 fb^{-1}
D4	10 GeV $\times$ 137 GeV eD, 100 fb^{-1}	P4	10 GeV $\times$ 275 GeV ep, 100 fb^{-1}
D5	18 GeV $\times$ 137 GeV eD, 15.4 fb^{-1}	P5	18 GeV $\times$ 275 GeV ep, 15.4 fb^{-1}
		P6	18 GeV $\times$ 275 GeV ep, 100 fb^{-1}

Additionally assume 70% hadron beam polarization, 80% electron beam polarization

- Allows us to study the interplay between high energy/low luminosity (for example, P5) versus low energy/high luminosity (for example, P4).
- Polarized deuteron and proton copies of these data sets are also studied, and labeled as ΔD, ΔP.
- Data sets where the lepton charge asymmetry is considered are labeled as LD, LP.

Observables at the EIC

- The ability to polarize both beams at the EIC, and potentially swap an electron beam for a positron beam, leads to a host of observables.

  - Polarized electrons, unpolarized hadrons: $$A_{\mathrm{PV}} = \frac{d\sigma_\ell}{d\sigma_0}$$
  - Unpolarized electrons, polarized hadrons: $$\Delta A_{\mathrm{PV}} = \frac{d\sigma_H}{d\sigma_0}$$
  - Lepton charge asymmetries: $$A_{\mathrm{LC}} = \frac{d\sigma_0(e^+H) - d\sigma_0(e^-H)}{d\sigma_0(e^+H) + d\sigma_0(e^-H)}$$

Observables studied: A^e_{PV}, ΔA^P_{PV}, ΔA^D_{PV}, A^P_{LC}, A^D_{LC}

Observables at the EIC

- The ability to polarize both beams at the EIC, and potentially swap an electron beam for a positron beam, leads to a host of observables.
  - Polarized electrons, unpolarized hadrons: $$A_{\mathrm{PV}} = \frac{d\sigma_\ell}{d\sigma_0}$$
  - Unpolarized electrons, polarized hadrons: $$\Delta A_{\mathrm{PV}} = \frac{d\sigma_H}{d\sigma_0}$$
  - Lepton charge asymmetries: $$A_{\mathrm{LC}} = \frac{d\sigma_0(e^+H) - d\sigma_0(e^-H)}{d\sigma_0(e^+H) + d\sigma_0(e^-H)}$$

Simulation details:

- Inelasticity cuts: y>0.1, y<0.9
- x<0.5, Q>10 GeV to avoid uncertainties from non-perturbative QCD and nuclear dynamics

Error budget example: unpolarized protons

- As an example of the expected EIC errors we will study the error budget for P5, the unpolarized high-energy proton scenario.
- Bins first ordered in Q^2. Within each Q^2 bin we then order in x; HL is a proposed high-luminosity option with an increase by a factor of 10 w.r.t the nominal integrated luminosity

RB, Emmert, Kutz, Mantry, Nycz, Petriello, Simsek, Wiegand, Zheng, 2022

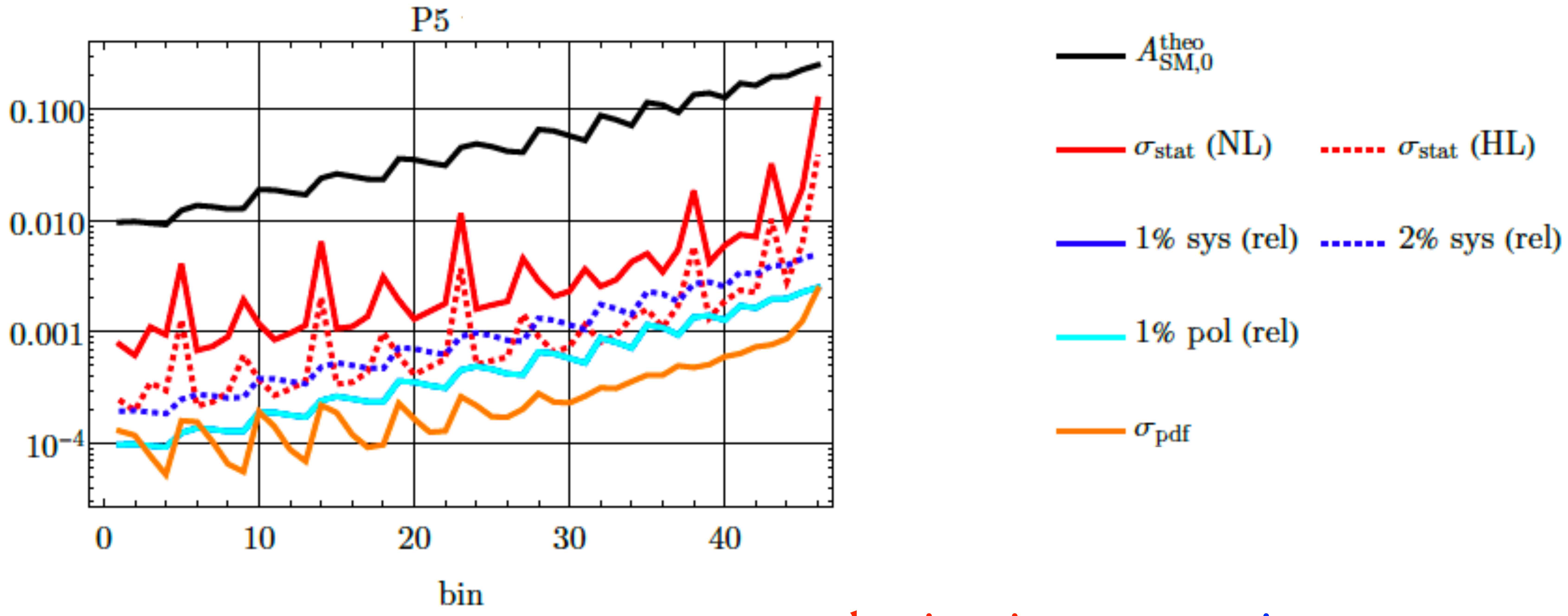

Statistical uncertainties dominant with nominal luminosity; systematic errors more relevant at high luminosity; PDF errors negligible. **Asymmetry much larger than all uncertainties.**

Single-parameter fits

- We will first consider the single-parameter fits, to understand the scales that can be probed at an EIC.

RB, Emmert, Kutz, Mantry, Nycz, Petriello, Simsek, Wiegand, Zheng, 2022

Note: lighter histograms obtained by fitting polarization uncertainty as a nuisance parameter in the fit; results in stronger constraints for polarized lepton cases

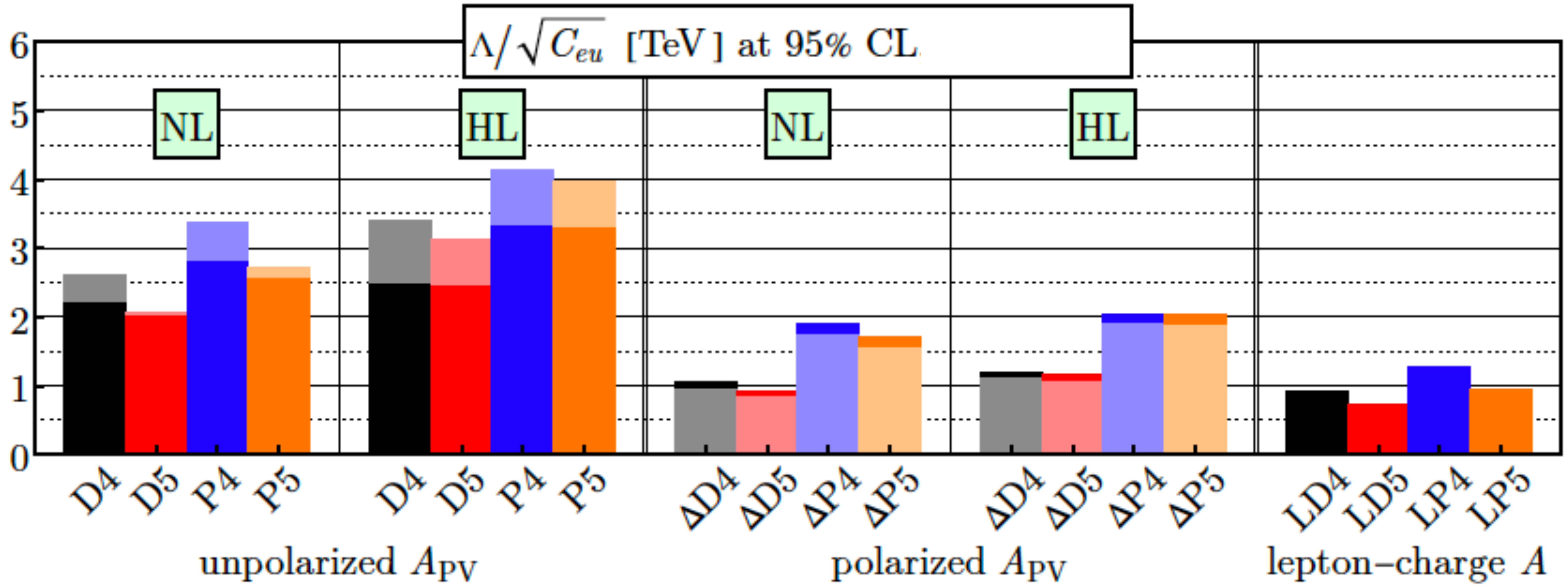

Trends:

- Proton sensitivities stronger than deuteron ones
- Unpolarized hadrons, polarized electrons offer strongest probes
- Lepton-charge asymmetries provide weakest probes

Single-parameter fits

- We will first consider the single-parameter fits, to understand the scales that can be probed at and EIC.

RB, Emmert, Kutz, Mantry, Nycz, Petriello, Simsek, Wiegand, Zheng, 2022

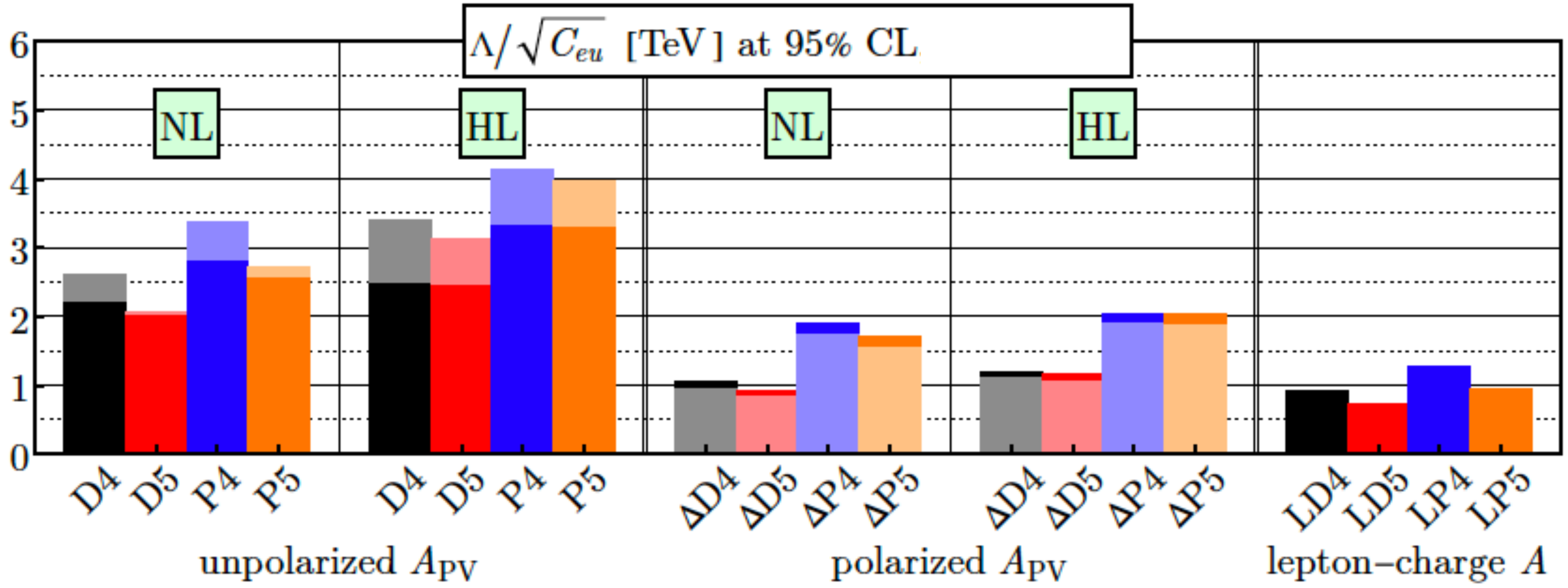

Up to 3 TeV scales probes with nominal luminosity, 4 TeV with high luminosity. Competitive with current LHC bounds.

Single-parameter fits

- We will first consider the single-parameter fits, to understand the scales that can be probed at and EIC.

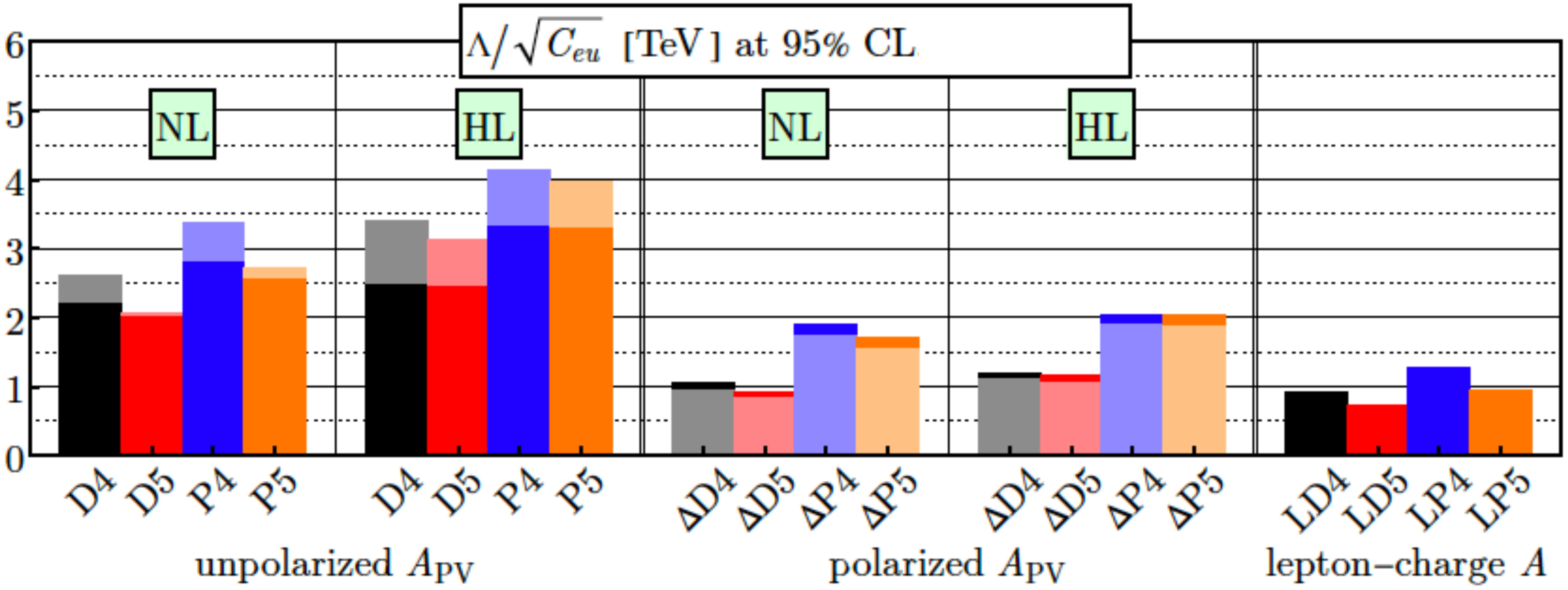

We have performed this study at dimension-6. Note that the $\Lambda/\sqrt{C}$ bounds are much greater than the momentum transfer Q<50 GeV. The expansion parameter $CQ^2/\Lambda^2 \ll 1$ unlike at the LHC, indicating that dim-8 is suppressed. Allows us to focus on dim-6 without contamination with dim-8!

Multi-parameter fits

- We can turn on more Wilson coefficients to test for degeneracies and check for degradation of the bounds. Only slightly weaker bounds in a 6-dimensional fit. The EIC can probe the full parameter space of semi-leptonic four-fermion Wilson coefficients.

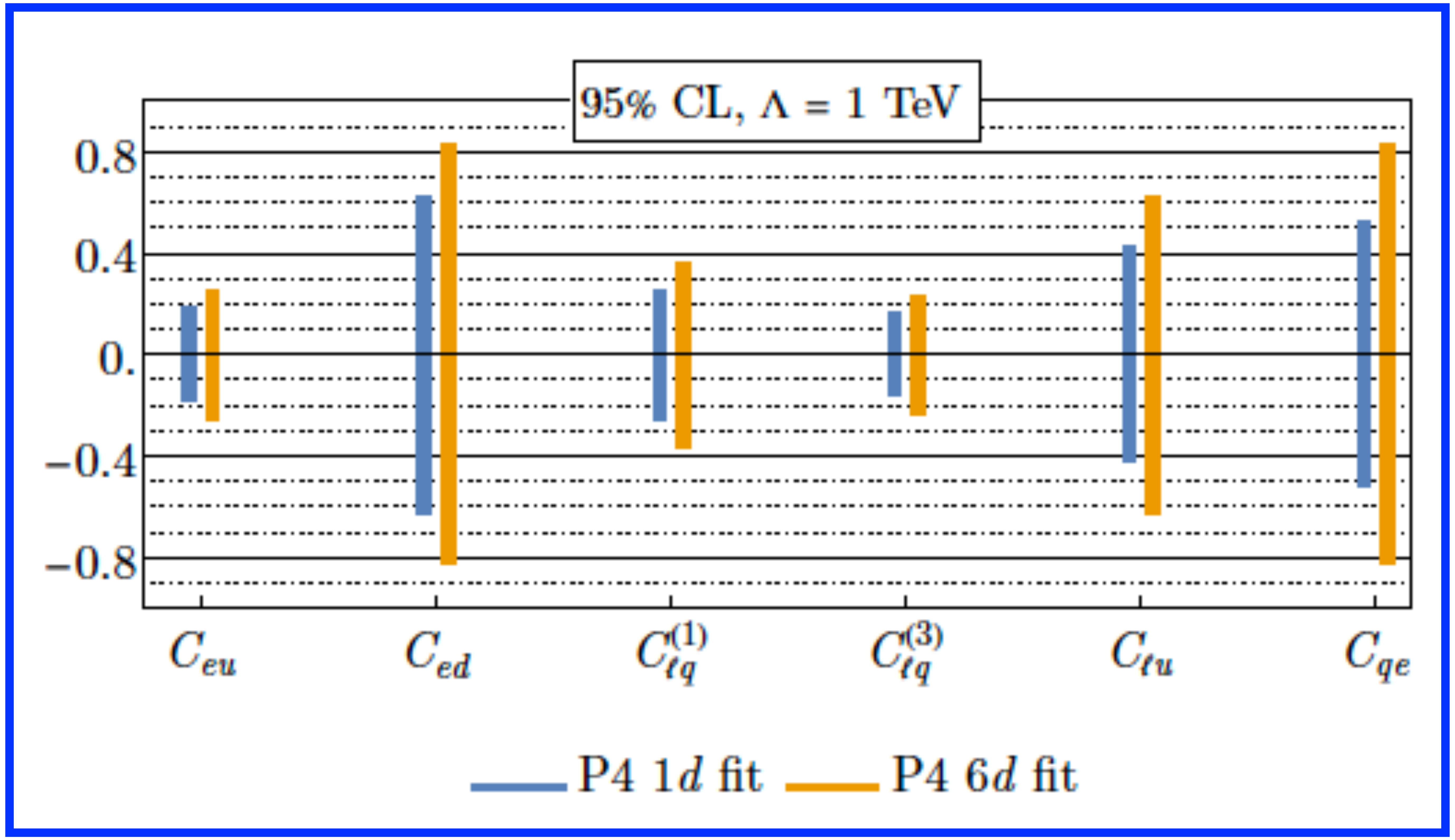

Compare to the LHC:

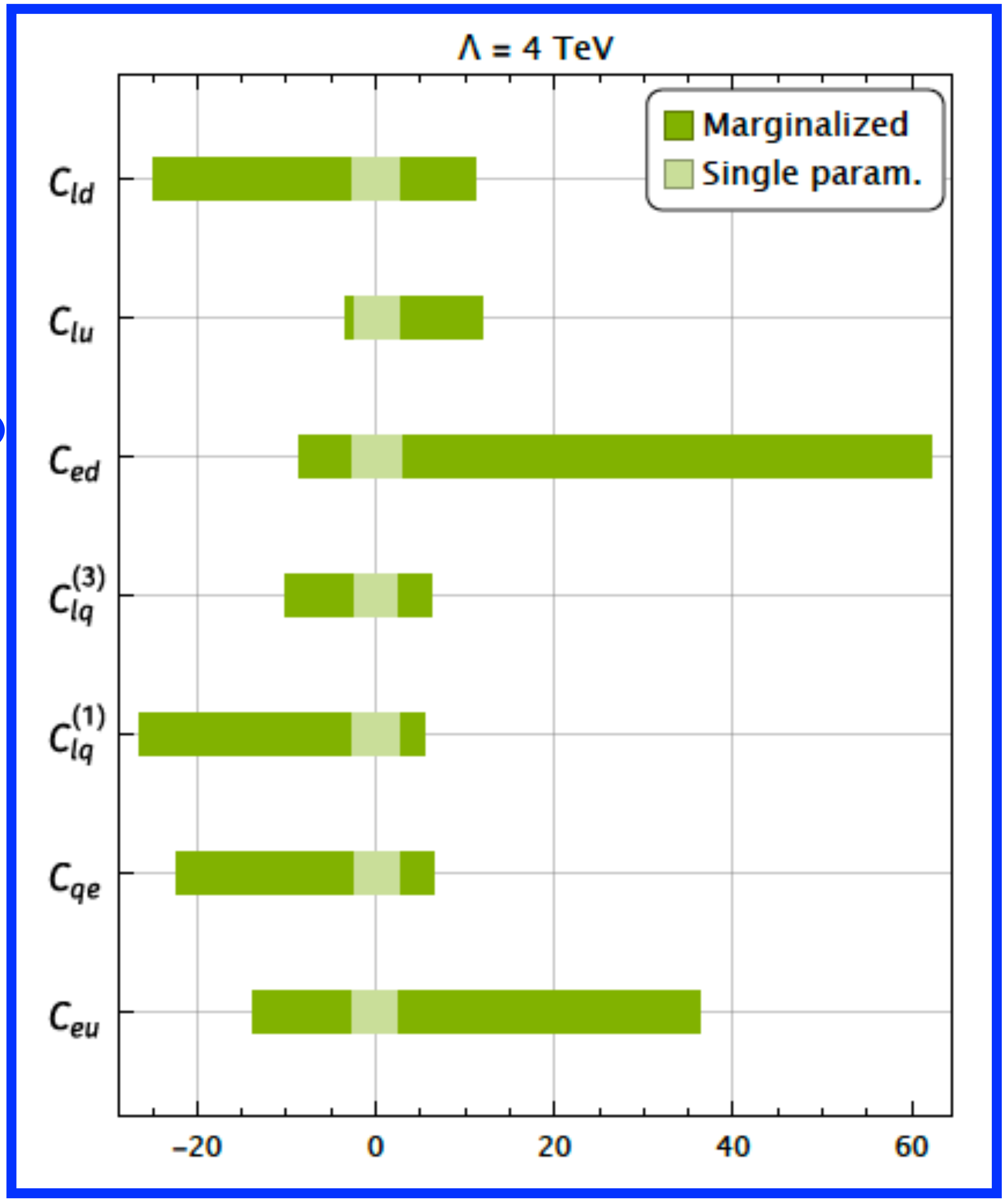

Future high-energy DIS experiments (LHeC/FCC-eh)

Comparison of future high-energy DIS machines

- Next we turn our attention to proposed future DIS machines such as the LHeC and the FCC-eh. We will compare the potential of the EIC with these future machines.

Experiment	Data set label	Data set configuration	Observable
LHeC	LHeC1	$60\text{ GeV}\times 1000\text{ GeV}\ e^-p,\ P_\ell=0,\ \mathcal{L}=100\text{ fb}^{-1}$	$\sigma_{\rm NC}$
	LHeC2	$60\text{ GeV}\times 7000\text{ GeV}\ e^-p,\ P_\ell=-80\%,\ \mathcal{L}=100\text{ fb}^{-1}$	
	LHeC3	$60\text{ GeV}\times 7000\text{ GeV}\ e^-p,\ P_\ell=+80\%,\ \mathcal{L}=30\text{ fb}^{-1}$	
	LHeC4	$60\text{ GeV}\times 7000\text{ GeV}\ e^+p,\ P_\ell=+80\%,\ \mathcal{L}=10\text{ fb}^{-1}$	
	LHeC5	$60\text{ GeV}\times 7000\text{ GeV}\ e^-p,\ P_\ell=-80\%,\ \mathcal{L}=1000\text{ fb}^{-1}$	
	LHeC6	$60\text{ GeV}\times 7000\text{ GeV}\ e^-p,\ P_\ell=+80\%,\ \mathcal{L}=300\text{ fb}^{-1}$	
	LHeC7	$60\text{ GeV}\times 7000\text{ GeV}\ e^+p,\ P_\ell=0\%,\ \mathcal{L}=100\text{ fb}^{-1}$	
FCC-eh	FCCeh1	$60\text{ GeV}\times 50000\text{ GeV}\ e^-p,\ P_\ell=-80\%,\ \mathcal{L}=2\text{ ab}^{-1}$	$\sigma_{\rm NC}$
	FCCeh2	$60\text{ GeV}\times 50000\text{ GeV}\ e^-p,\ P_\ell=+80\%,\ \mathcal{L}=0.5\text{ ab}^{-1}$	
	FCCeh3	$60\text{ GeV}\times 50000\text{ GeV}\ e^+p,\ P_\ell=0,\ \mathcal{L}=0.2\text{ ab}^{-1}$	
EIC	D4	$10\text{ GeV}\times 137\text{ GeV}\ e^-D,\ P_\ell=80\%,\ \mathcal{L}=100\text{ fb}^{-1}$	$A_{\rm PV}$
	D5	$18\text{ GeV}\times 137\text{ GeV}\ e^-D,\ P_\ell=80\%,\ \mathcal{L}=15.4\text{ fb}^{-1}$	
	P4	$10\text{ GeV}\times 275\text{ GeV}\ e^-p,\ P_\ell=80\%,\ \mathcal{L}=100\text{ fb}^{-1}$	
	P5	$18\text{ GeV}\times 275\text{ GeV}\ e^-p,\ P_\ell=80\%,\ \mathcal{L}=15.4\text{ fb}^{-1}$	
	ΔD4	The same as D4 but with $P_\ell=0$ and $P_H=70\%$	$\Delta A_{\rm PV}$
	ΔD5	The same as D5 but with $P_\ell=0$ and $P_H=70\%$	
	ΔP4	The same as P4 but with $P_\ell=0$ and $P_H=70\%$	
	ΔP5	The same as P5 but with $P_\ell=0$ and $P_H=70\%$	

Britzger, Klein, Spiesberger (2020-2022)

← Note different polarizations, lepton species (e+ vs e-).

LHeC, FCC-eh run scenarios taken from the literature. All three machines feature high luminosity, polarization

Error budgets for LHeC, FCC-eh

- Both future machines will be limited by systematic errors (purple lines in the plots below). Note that the estimated PDF errors (orange lines) are equal to or less than the systematic errors in most phase space. NLO QCD is included, error from NNLO negligible.

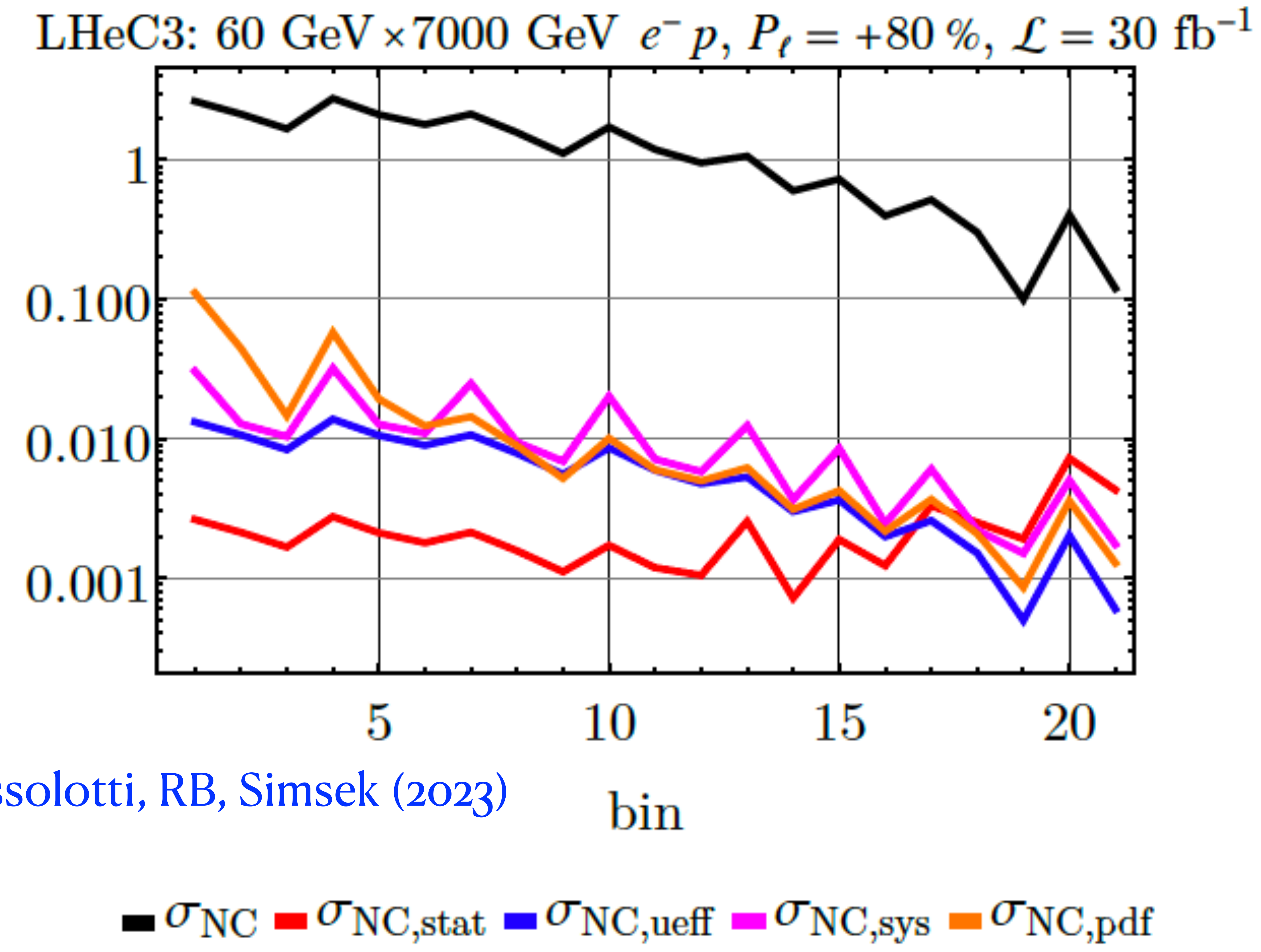

Bissolotti, RB, Simsek (2023)

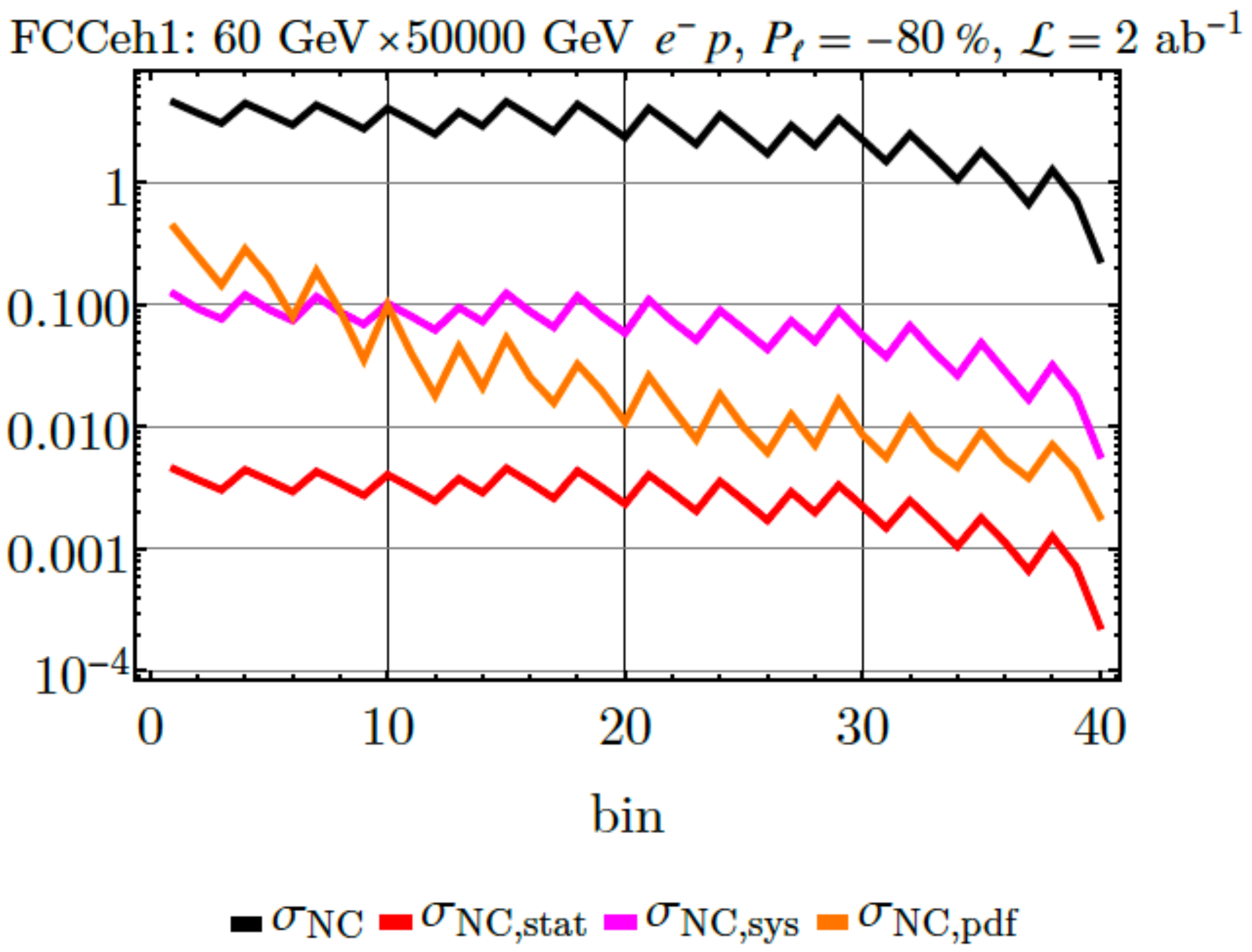

Marginalized constraints

- Note that future machines do not suffer from parameter space degeneracies like the LHC. To show this we focus on an example where the SMEFT corrections to three run scenarios (LHeC2, LHeC4, LHeC5) approximately vanish, still focusing on four-fermion interactions.

Bissolotti, RB, Simsek (2023)

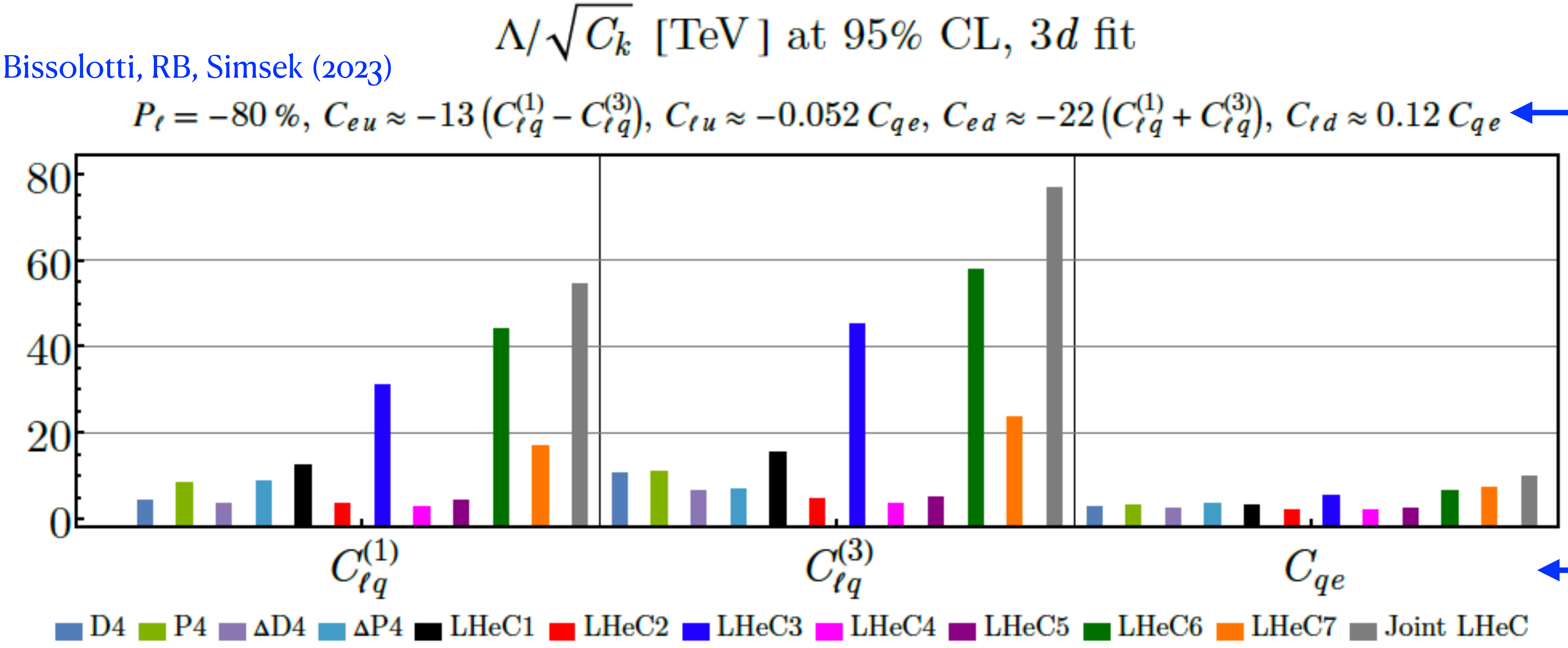

Fix these four; numbers come from combinations of SM EW couplings and correspond to the LHeC degeneracy

Fit these three

Marginalized constraints

Bissolotti, RB, Simsek (2023)

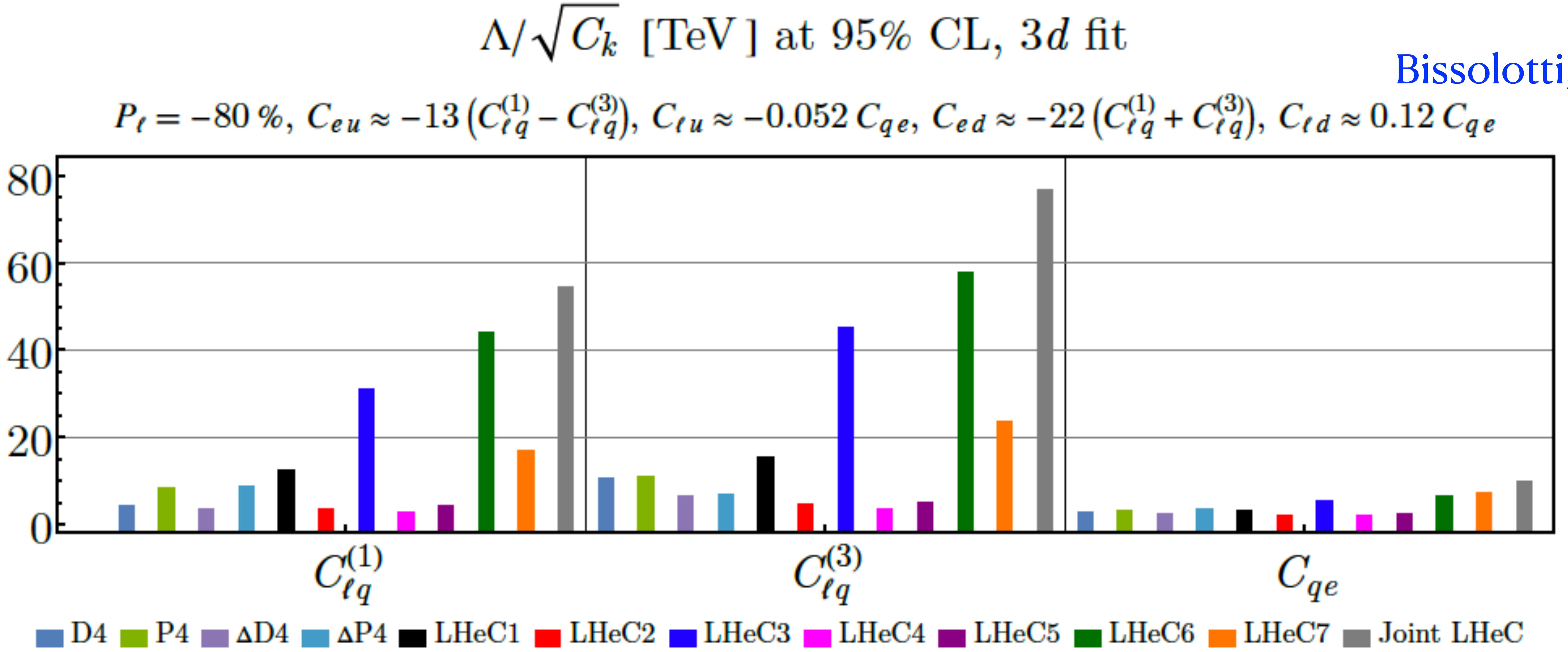

- Combined bounds on the effective UV scale from all LHeC runs reach at least 10 TeV for all three coefficients, 70 TeV for the strongest.
- **Note**: the effective UV scale probed is greater than the 1-1.5 TeV momentum transfer reached by these experiments; EFT expansion is valid and appropriate.
- Need all polarization, lepton species to cover the parameter space! No single LHeC run is the strongest for all three parameters.
- Not surprisingly, combined LHeC (and FCC-eh) bounds are far stronger than EIC bounds; higher energy and integrated luminosity.

Electroweak precision constraints

- The power of these future machines is so strong that we can improve upon the existing precision constraints on the ffV vertices driven primarily by LEP and SLC.

ffV		semi-leptonic four-fermion	
$C_{\varphi WB}$	$O_{\varphi WB} = (\varphi^\dagger \tau^I \varphi) W^I_{\mu\nu} B^{\mu\nu}$	$C^{(1)}_{\ell q}$	$O^{(1)}_{\ell q} = (\bar{\ell}\gamma_\mu \ell)(\bar{q}\gamma^\mu q)$
$C_{\varphi D}$	$O_{\varphi D} = (\varphi^\dagger D_\mu \varphi)^* (\varphi^\dagger D^\mu \varphi)$	$C^{(3)}_{\ell q}$	$(\bar{\ell}\gamma_\mu \tau^I \ell)(\bar{q}\gamma^\mu \tau^I q)$
$C^{(1)}_{\varphi \ell}$	$O^{(1)}_{\varphi \ell} = (\varphi^\dagger i \overleftrightarrow{D}_\mu \varphi)(\bar{\ell}\gamma^\mu \ell)$	C_{eu}	$O_{eu} = (\bar{e}\gamma_\mu e)(\bar{u}\gamma^\mu u)$
$C^{(3)}_{\varphi \ell}$	$O^{(3)}_{\varphi \ell} = (\varphi^\dagger i \overleftrightarrow{D}_\mu \tau^I \varphi)(\bar{\ell}\gamma^\mu \tau^I \ell)$	C_{ed}	$O_{ed} = (\bar{e}\gamma_\mu e)(\bar{d}\gamma^\mu d)$
$C_{\varphi e}$	$O_{\varphi e} = (\varphi^\dagger i \overleftrightarrow{D}_\mu \varphi)(\bar{e}\gamma^\mu e)$	$C_{\ell u}$	$O_{\ell u} = (\bar{\ell}\gamma_\mu \ell)(\bar{u}\gamma^\mu u)$
$C^{(1)}_{\varphi q}$	$O^{(1)}_{\varphi q} = (\varphi^\dagger i \overleftrightarrow{D}_\mu \varphi)(\bar{q}\gamma^\mu q)$	$C_{\ell d}$	$O_{\ell d} = (\bar{\ell}\gamma_\mu \ell)(\bar{d}\gamma^\mu d)$
$C^{(3)}_{\varphi q}$	$O^{(3)}_{\varphi q} = (\varphi^\dagger i \overleftrightarrow{D}_\mu \tau^I \varphi)(\bar{q}\gamma^\mu \tau^I q)$	C_{qe}	$O_{qe} = (\bar{q}\gamma_\mu q)(\bar{e}\gamma^\mu e)$
$C_{\varphi u}$	$O_{\varphi u} = (\varphi^\dagger i \overleftrightarrow{D}_\mu \varphi)(\bar{u}\gamma^\mu u)$		
$C_{\varphi d}$	$O_{\varphi d} = (\varphi^\dagger i \overleftrightarrow{D}_\mu \varphi)(\bar{d}\gamma^\mu d)$		
$C_{\ell\ell}$	$O_{\ell\ell} = (\bar{\ell}\gamma_\mu \ell)(\bar{\ell}\gamma^\mu \ell)$		

We turn on the full 17 operators that contribute to DIS at tree-level in the EW couplings

Electroweak precision constraints

- The power of these future machines is so strong that we can improve upon the existing precision constraints on there ffV vertices driven primarily by LEP and SLC.

ffV		semi-leptonic four-fermion	
$C_{\varphi WB}$	$O_{\varphi WB} = (\varphi^\dagger \tau^I \varphi) W^I_{\mu\nu} B^{\mu\nu}$	$C^{(1)}_{\ell q}$	$O^{(1)}_{\ell q} = (\bar{\ell}\gamma_\mu \ell)(\bar{q}\gamma^\mu q)$
$C_{\varphi D}$	$O_{\varphi D} = (\varphi^\dagger D_\mu \varphi)^* (\varphi^\dagger D^\mu \varphi)$	$C^{(3)}_{\ell q}$	$(\bar{\ell}\gamma_\mu \tau^I \ell)(\bar{q}\gamma^\mu \tau^I q)$
$C^{(1)}_{\varphi \ell}$	$O^{(1)}_{\varphi \ell} = (\varphi^\dagger i \overleftrightarrow{D}_\mu \varphi)(\bar{\ell}\gamma^\mu \ell)$	C_{eu}	$O_{eu} = (\bar{e}\gamma_\mu e)(\bar{u}\gamma^\mu u)$
$C^{(3)}_{\varphi \ell}$	$O^{(3)}_{\varphi \ell} = (\varphi^\dagger i \overleftrightarrow{D}_\mu \tau^I \varphi)(\bar{\ell}\gamma^\mu \tau^I \ell)$	C_{ed}	$O_{ed} = (\bar{e}\gamma_\mu e)(\bar{d}\gamma^\mu d)$
$C_{\varphi e}$	$O_{\varphi e} = (\varphi^\dagger i \overleftrightarrow{D}_\mu \varphi)(\bar{e}\gamma^\mu e)$	$C_{\ell u}$	$O_{\ell u} = (\bar{\ell}\gamma_\mu \ell)(\bar{u}\gamma^\mu u)$
$C^{(1)}_{\varphi q}$	$O^{(1)}_{\varphi q} = (\varphi^\dagger i \overleftrightarrow{D}_\mu \varphi)(\bar{q}\gamma^\mu q)$	$C_{\ell d}$	$O_{\ell d} = (\bar{\ell}\gamma_\mu \ell)(\bar{d}\gamma^\mu d)$
$C^{(3)}_{\varphi q}$	$O^{(3)}_{\varphi q} = (\varphi^\dagger i \overleftrightarrow{D}_\mu \tau^I \varphi)(\bar{q}\gamma^\mu \tau^I q)$	C_{qe}	$O_{qe} = (\bar{q}\gamma_\mu q)(\bar{e}\gamma^\mu e)$
$C_{\varphi u}$	$O_{\varphi u} = (\varphi^\dagger i \overleftrightarrow{D}_\mu \varphi)(\bar{u}\gamma^\mu u)$		
$C_{\varphi d}$	$O_{\varphi d} = (\varphi^\dagger i \overleftrightarrow{D}_\mu \varphi)(\bar{d}\gamma^\mu d)$		
$C_{\ell\ell}$	$O_{\ell\ell} = (\bar{\ell}\gamma_\mu \ell)(\bar{\ell}\gamma^\mu \ell)$		

Existing single-parameter constraints on the ffV Wilson coefficients are quite strong; can future DIS experiments improve upon these?

Dawson, Giardino (2019)

C_k	95% CL, $\Lambda = 1$ TeV
$C^{(1)}_{\varphi\ell}$	$[-0.043, 0.012]$
$C^{(3)}_{\varphi\ell}$	$[-0.012, 0.0029]$
$C_{\varphi e}$	$[-0.013, 0.0094]$
$C^{(1)}_{\varphi q}$	$[-0.027, 0.043]$
$C^{(3)}_{\varphi q}$	$[-0.011, 0.014]$
$C_{\varphi u}$	$[-0.072, 0.091]$
$C_{\varphi d}$	$[-0.16, 0.060]$
$C_{\varphi WB}$	$[-0.0088, 0.0013]$

Electroweak precision constraints

- We consider the full 17-dim marginalized fit and show 2-dim projections below for all three machines: EIC, LHeC, FCC-eh. We take the EWPO fit from J.Ellis et al (2012.02779).

Bissolotti, RB Simsek (2023)

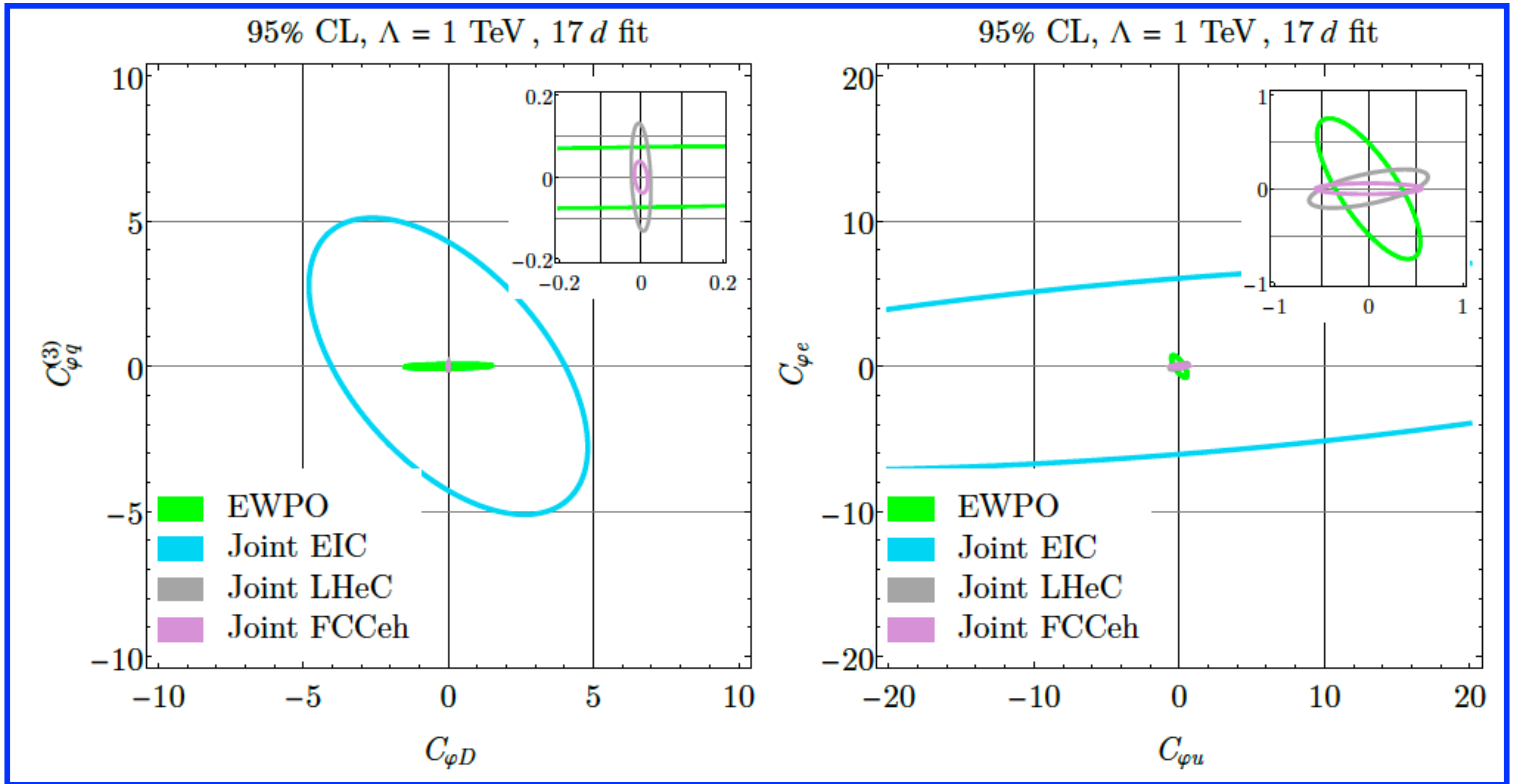

Two example projections of the full 17-dim fit. The FCC-eh can significantly improve on EWPO constraints!

Highlights from the BNL EIC workshop

Uncovering New Laws of Nature, Nov 20-22, 2024

Joint SMEFT+PDF fits

- It is possible that the effects of heavy new physics can be absorbed into PDFs when fitting DY data. What are the implications of this issue at a future HL-LHC?

Perform a "Contamination test":

1. Choose a BSM model and a "true PDF" set
2. Produce BSM pseudodata
3. Fit PDFs on pseudodata assuming SM
4. Compare results with baseline PDFs (no BSM physics)

[2307.10370]

$$\mathcal{L}^{W}_{UV} = \mathcal{L}_{SM} - \frac{1}{4}W'^{a}_{\mu\nu}W'^{a,\mu\nu} + \frac{1}{2}M^2_{W'}W'^{a}_{\mu}W'^{a,\mu} - g_{W'}W'^{a,\mu}\sum_{f_L}\bar{f}_L T^a\gamma^\mu f_L$$

↓

$$\mathcal{L}^{W'}_{SMEFT} = \mathcal{L}_{SM} - \frac{g^2_{W'}}{2M^2_{W'}}J^{a,\mu}_{L}J^{a}_{L,\mu}$$

$$J^{a,\mu}_{L} = \sum_{f_L}\bar{f}_L T^a\gamma^\mu f_L$$

➡ Impacts Drell-Yan

HL-LHC Projections

E. Hammou, *Uncovering New Laws of Nature* (BNL, Nov. 2024)

Joint SMEFT+PDF fits

- It is possible that the effects of heavy new physics can be absorbed into PDFs when fitting DY data. What are the implications of this issue at a future HL-LHC?

Impact of contamination on predictions for other sectors

Theory predictions (red band):

- BSM PDFs + SM

Data (blue dots):

- True PDFs + SM

➡ Fake deviation from SM

Also seen in WH, WZ, ZH production

HL-LHC Projections

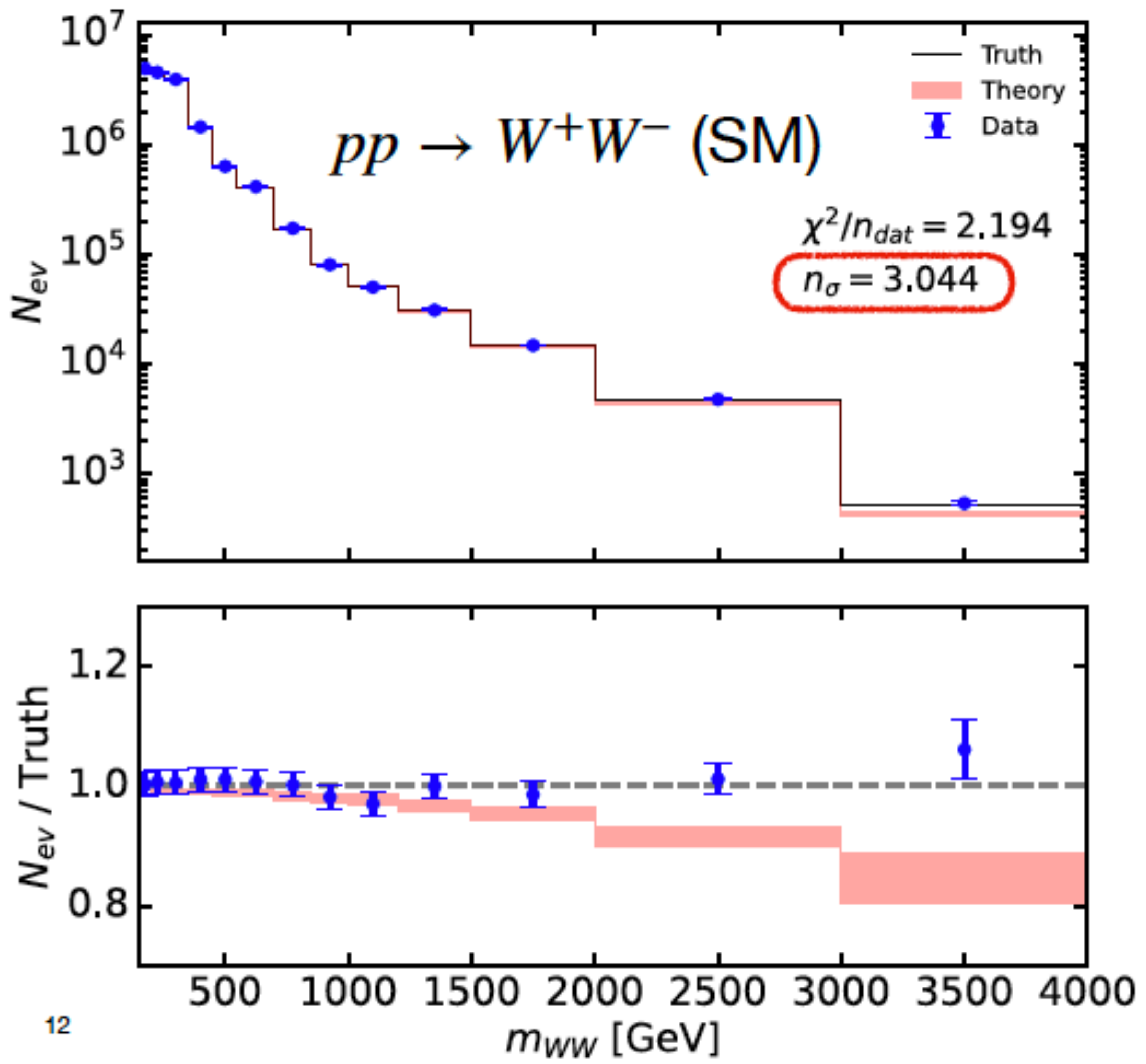

Having BSM absorbed into PDFs can fake new physics at the HL-LHC!

E. Hammou, *Uncovering New Laws of Nature* (BNL, Nov. 2024)

SMEFT and PDFs with EIC data

- Including EIC data in PDF fits can help avoid absorbing BSM effects into PDFs.

$$\hat{\sigma}_{BSM} \otimes \mathscr{L}_{SM} \approx \hat{\sigma}_{SM} \otimes \mathscr{L}_{BSM}$$

↓

$$\hat{\sigma}_{BSM} \otimes \mathscr{L}_{SM} \neq \hat{\sigma}_{SM} \otimes \mathscr{L}_{EIC+FPF}$$

$M_{W'}$: 13.8 TeV

FPF: forward proton facility

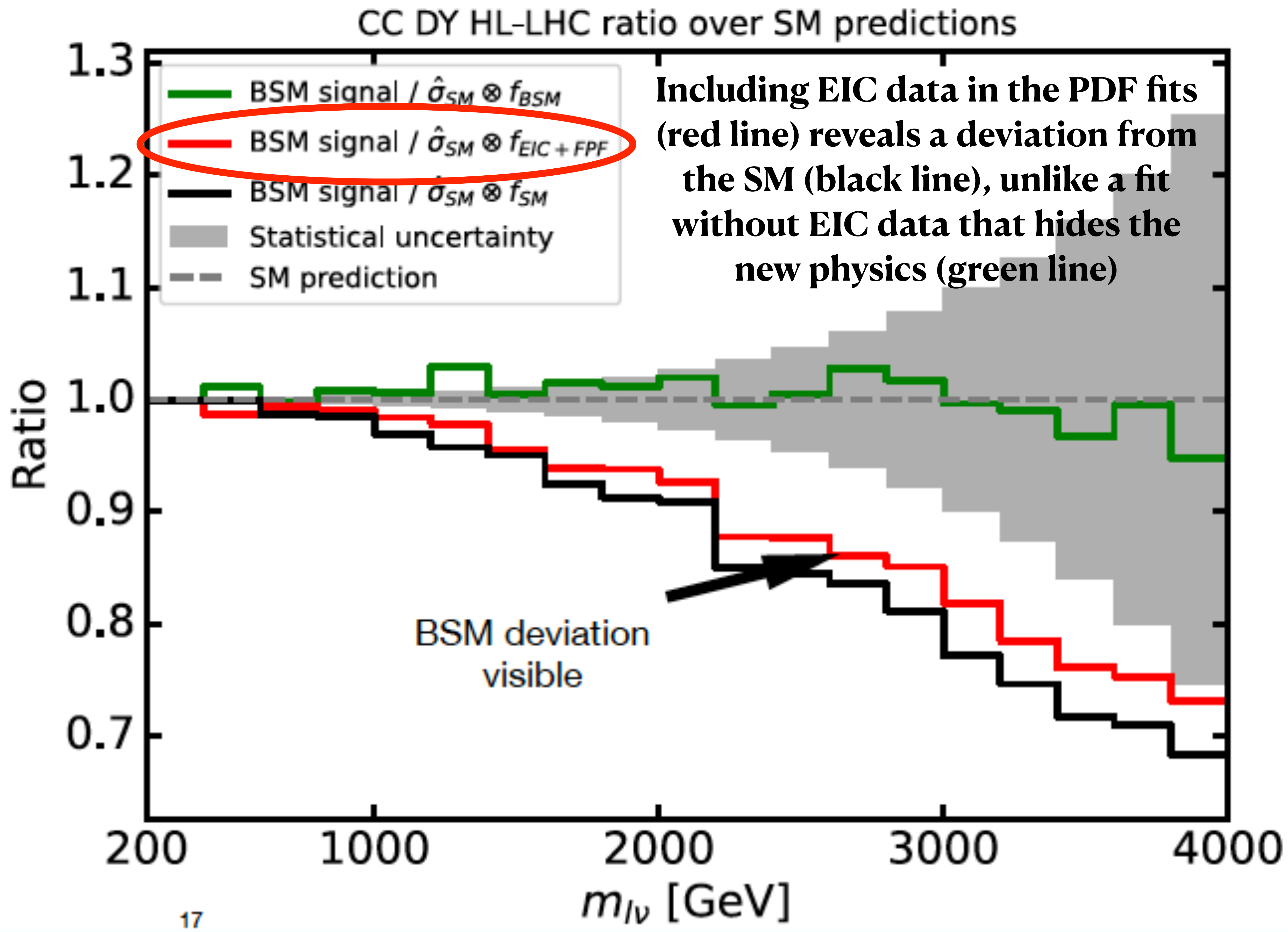

17

E. Hammou, *Uncovering New Laws of Nature* (BNL, Nov. 2024)

Conclusions

- The current experimental landscape suggests that the coming decade will require increasingly precise indirect searches in order to find hints of deviation from the SM.
- The SMEFT framework is ideal for organizing and interpreting these searches.
- The EIC is capable of powerful indirect probes of BSM effects difficult to access at the LHC due to its ability to polarize both beams.
- We have shown that the EIC can remove degeneracies in the four-fermion sector of the SMEFT that the LHC cannot distinguish.
- LHeC and FCCeH will further advance searches for heavy new physics.
- Looking forward to a rich and exciting future DIS program!

Back up

LHeC: a future high-energy DIS experiment

- **LHeC** (updated CDR: 2007.14491): a potential future high-energy DIS experiment based on the existing LHC experiment

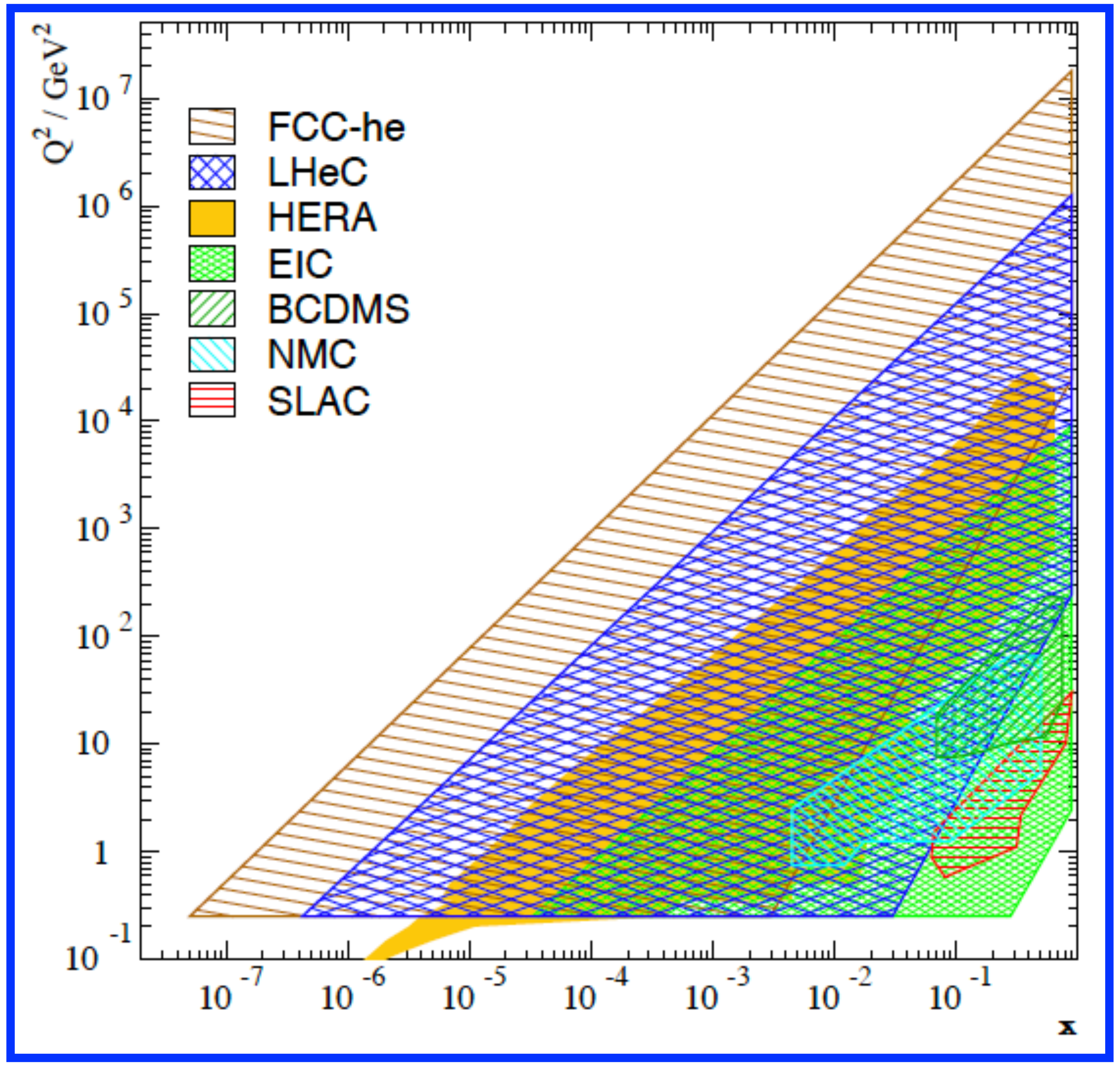

- Would feature a 50 GeV electron beam scattering off existing LHC proton/ion beams with a center-of mass energy reaching 1.5 TeV; concurrent operation with HL-LHC possible
- The integrated luminosity of such a machine could reach 1000 fb^{-1}
- Momentum transfers exceeding 1 TeV
- Increased coverage in the (x,Q^2) plane
- The possibility of polarizing the proton beam isn't considered, since the LHeC will reuse the LHC beam

FCC-eh: a second future high-energy DIS experiment

- **FCC-eh**: a proposed DIS experiment based upon a future circular collider complex at CERN

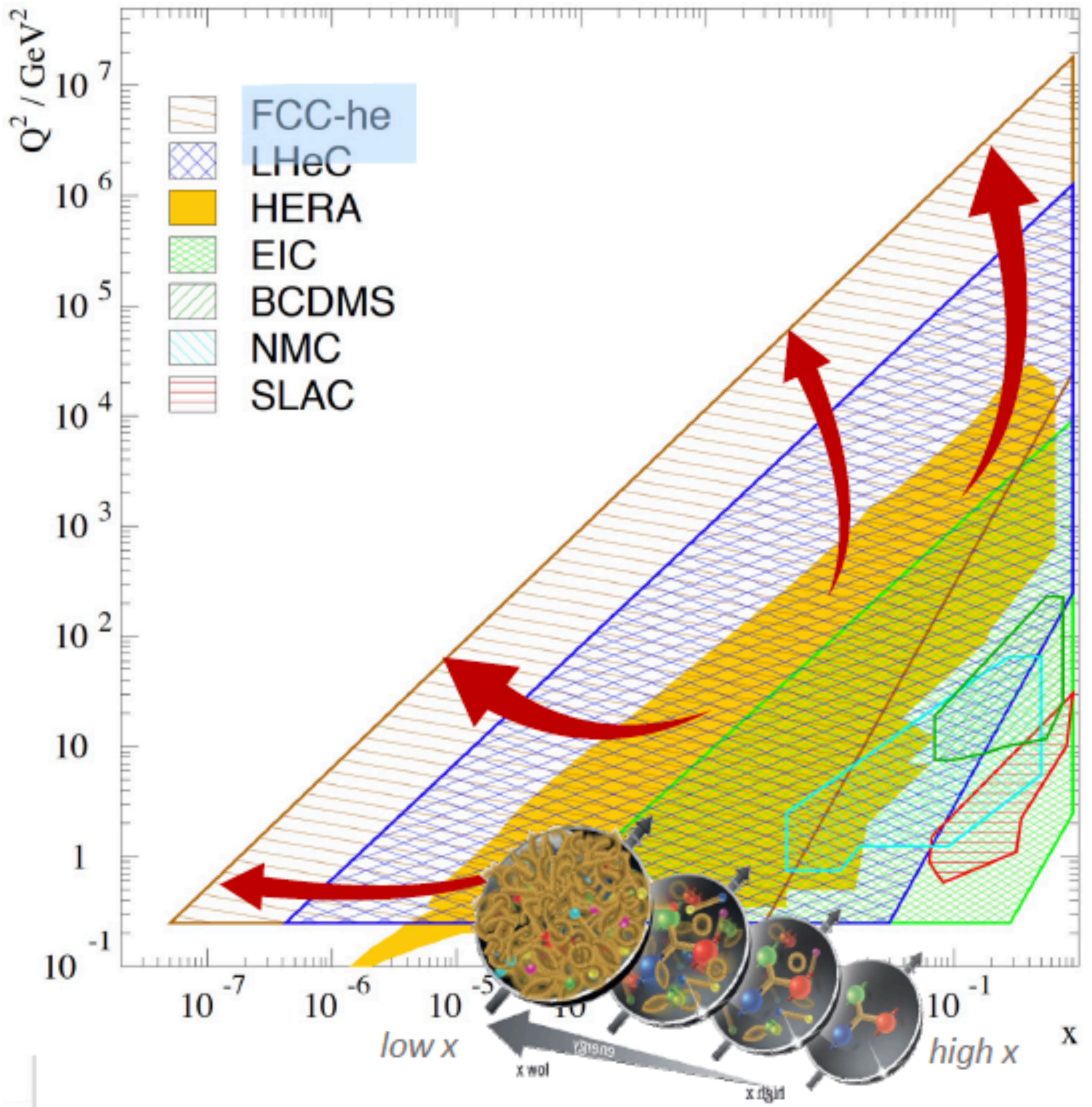

- Features a 60 GeV electron beam leading to a center-of mass energy of 3.5 TeV
- Up to several inverse attobarns of integrated luminosity
- Momentum transfers reaching 1.5 TeV
- Increased coverage in the (x,Q^2) plane